

Particle production and collectivity from small to large collision systems

A. Dobrin (Institute of Space Science – INFLPR subsidiary)

alexandru.florin.dobrin@cern.ch

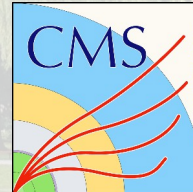
for the LHC Collaborations



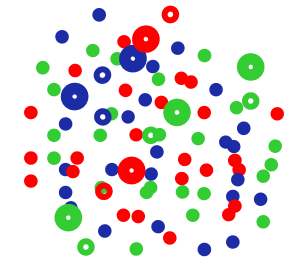
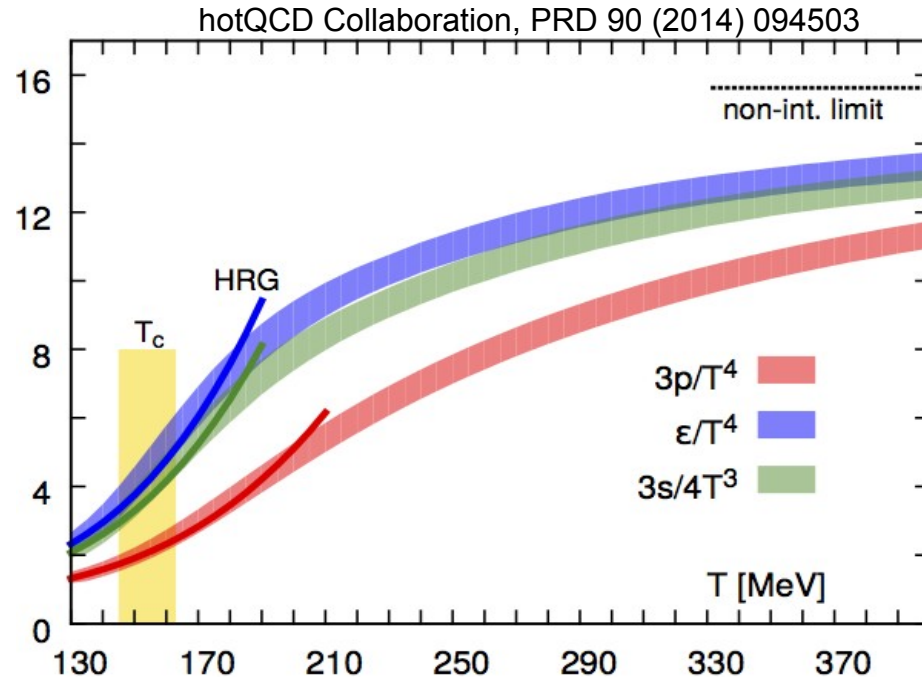
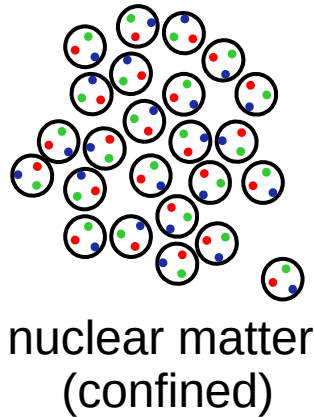
ALICE



ATLAS
EXPERIMENT



Lattice QCD: quark–gluon plasma (QGP)



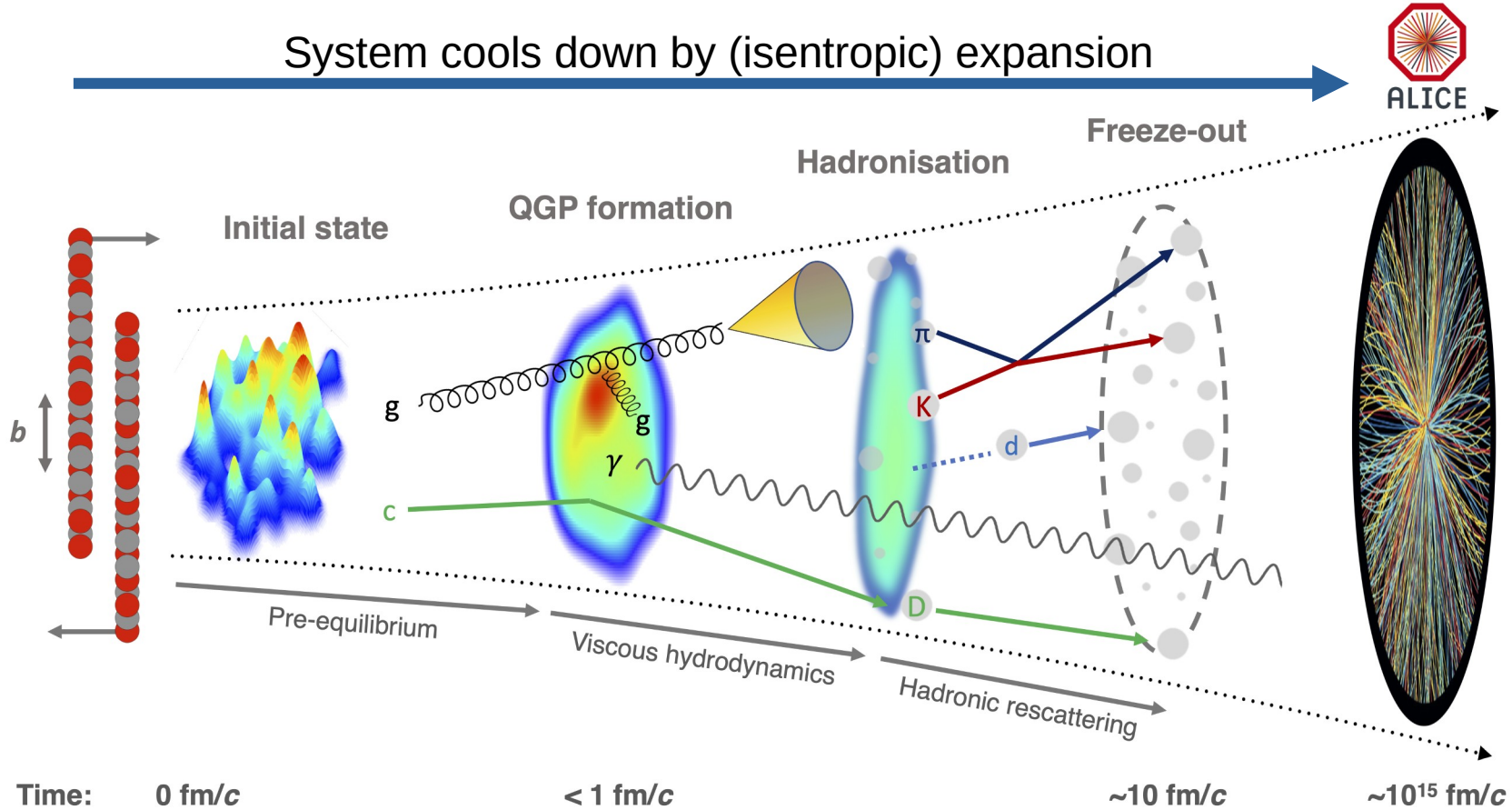
QGP
(deconfined)

$$p = \frac{1}{3} \epsilon = g \frac{\pi^2}{90} T^4$$

$$\frac{\epsilon}{T^4} = g \frac{\pi^2}{30}$$

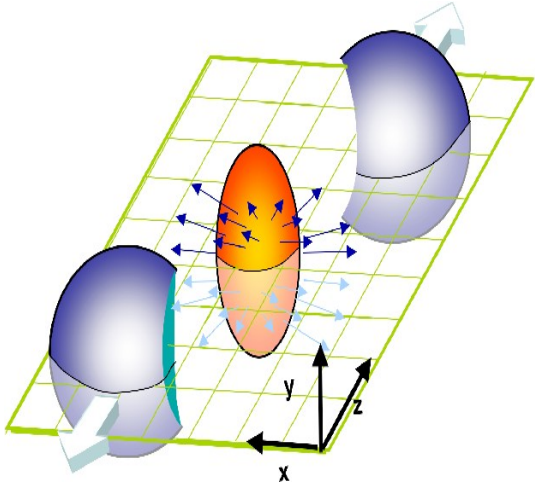
- Heating + compression → quark–gluon plasma (QGP): deconfined system of quarks and gluons
- Lattice QCD: transition expected to occur at energy density $\epsilon \sim 0.5 \text{ GeV}/\text{fm}^3$ and temperature $T \sim 156 \text{ MeV}$
 - Conditions achieved in laboratory by colliding heavy ions

Heavy-ion collisions: quark–gluon plasma (QGP)

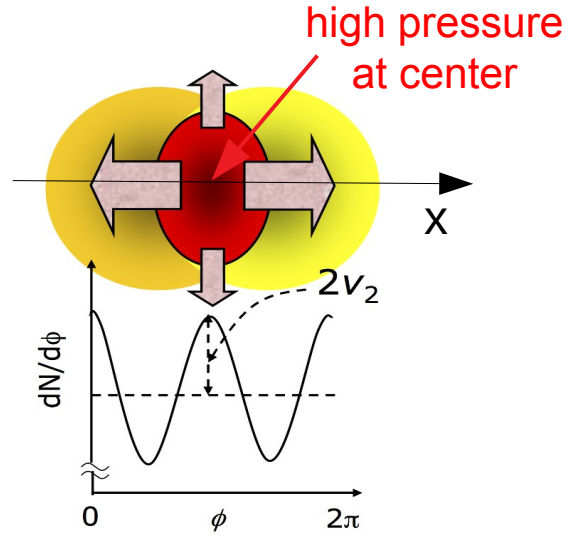
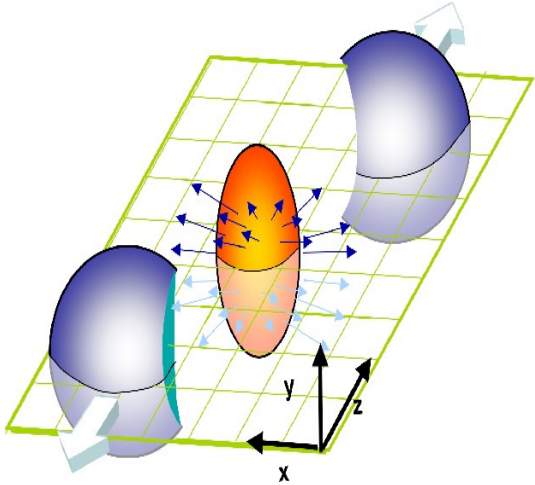


ALICE, arXiv:2211.04384

Anisotropic flow

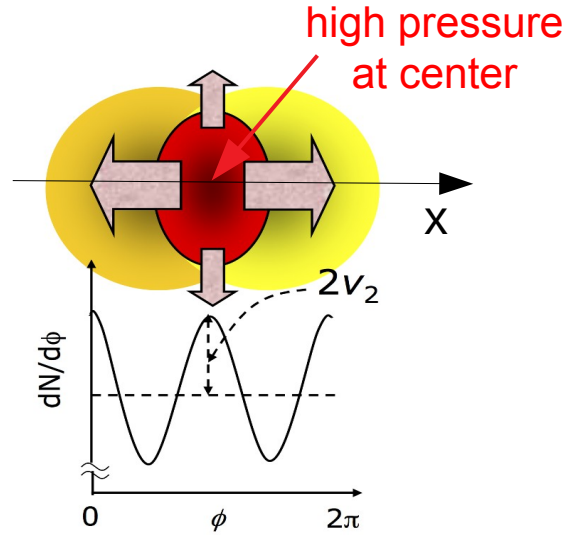
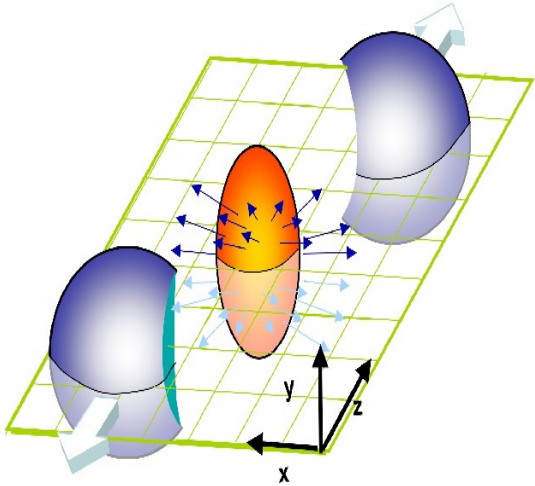


Anisotropic flow



Pressure gradients (larger in the x direction) push bulk “out” → “flow”
 More particles seen in the x-direction

Anisotropic flow

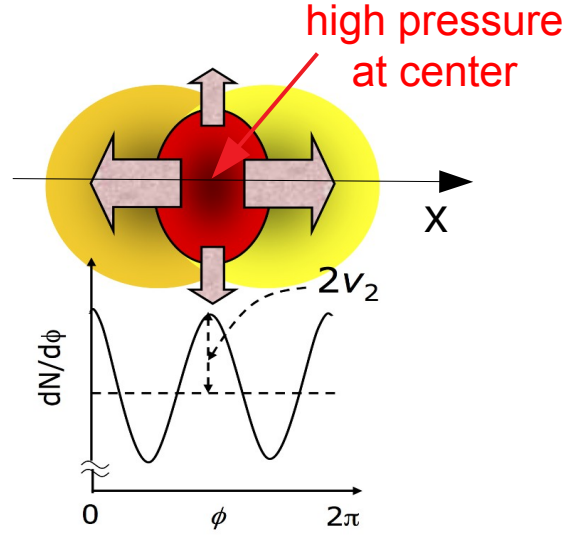
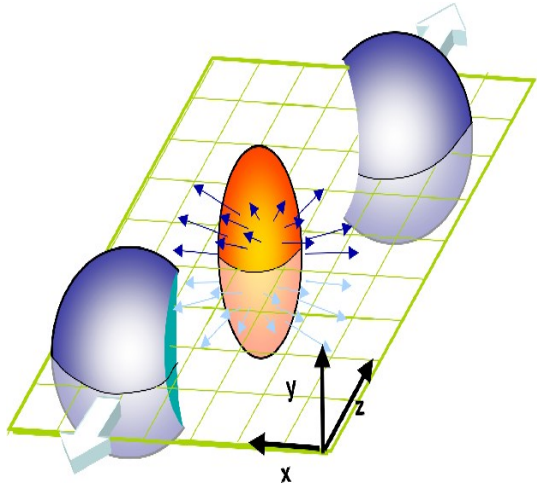


Pressure gradients (larger in the x direction) push bulk “out” → “flow”
 More particles seen in the x-direction

$$E \frac{d^3 N}{d^3 p} = \frac{1}{2\pi} \frac{d^2 N}{p_T d p_T d y} \left(1 + \sum_{n=1}^{\infty} 2 v_n \cos(n(\varphi - \Psi_n)) \right)$$

- **Anisotropic flow**: initial spatial anisotropy → final momentum anisotropy via collective interactions

Anisotropic flow



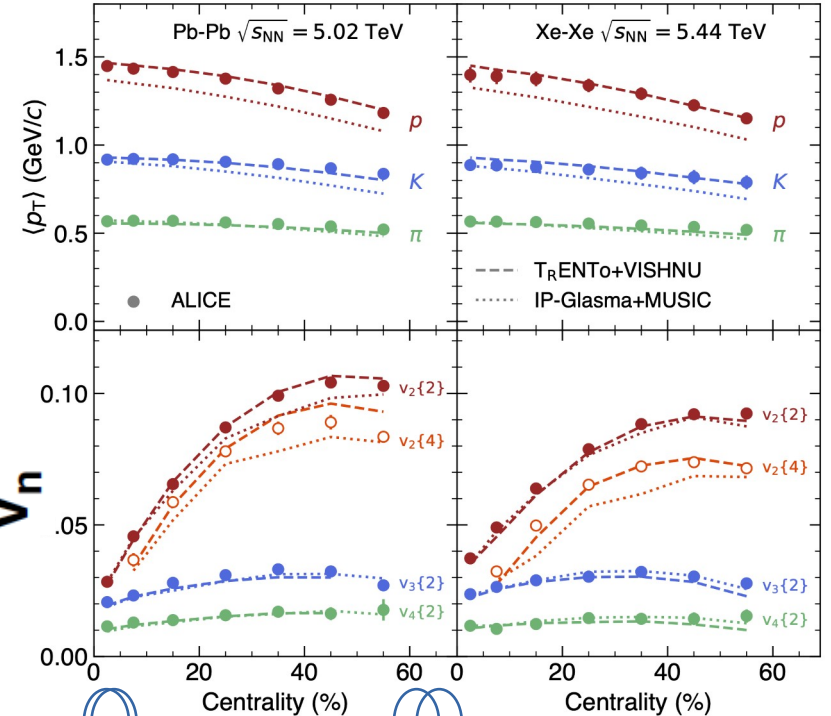
Pressure gradients (larger in the x direction) push bulk “out” → “flow”
 More particles seen in the x-direction

$$E \frac{d^3 N}{d^3 p} = \frac{1}{2\pi} \frac{d^2 N}{p_T d p_T d y} \left(1 + \sum_{n=1}^{\infty} 2v_n \cos(n(\varphi - \Psi_n)) \right)$$

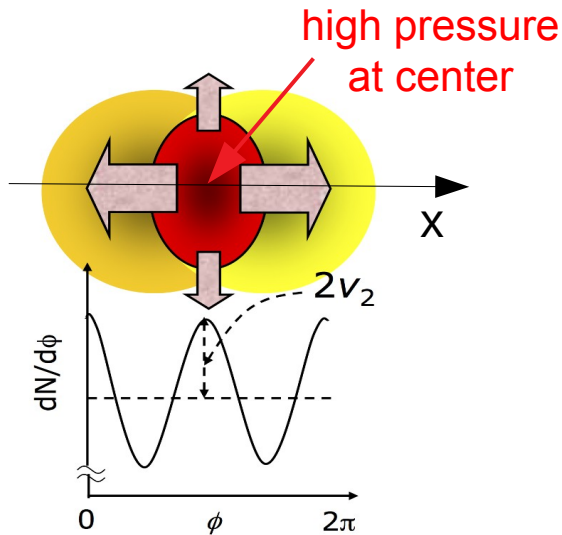
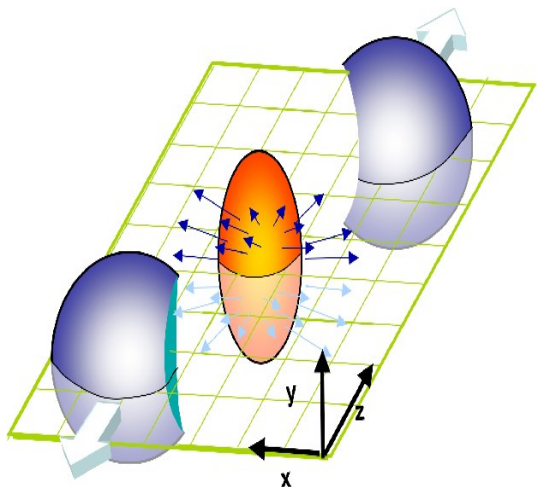
- **Anisotropic flow**: initial spatial anisotropy → final momentum anisotropy via collective interactions
 - v_n quantify the event anisotropy

v_n

ALICE, arXiv:2211.04384



Anisotropic flow



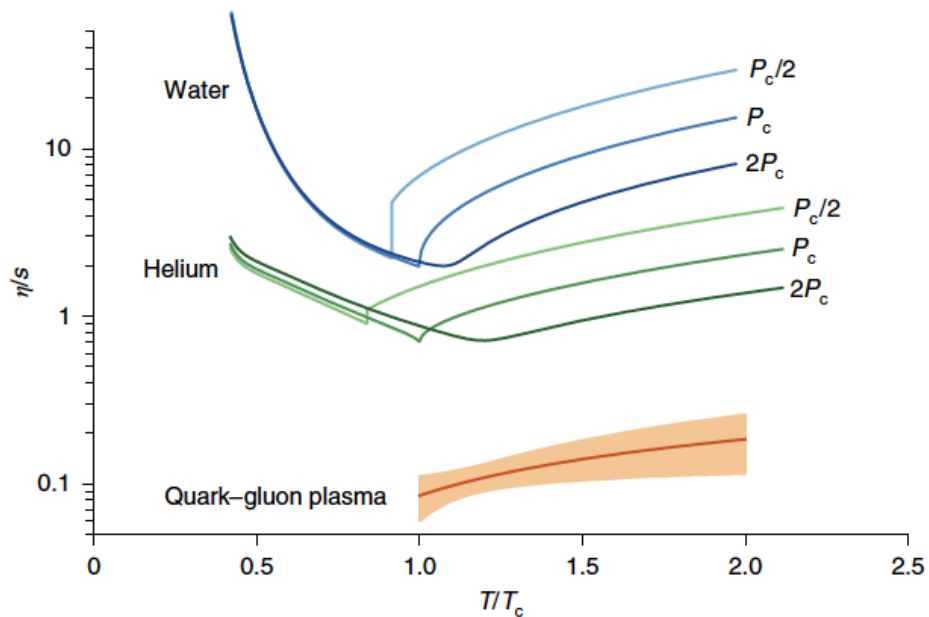
Pressure gradients (larger in the x direction) push bulk “out” → “flow”

More particles seen in the x-direction

$$E \frac{d^3 N}{d^3 p} = \frac{1}{2\pi} \frac{d^2 N}{p_T dp_T dy} \left(1 + \sum_{n=1}^{\infty} 2 v_n \cos(n(\varphi - \Psi_n)) \right)$$

- **Anisotropic flow**: initial spatial anisotropy → final momentum anisotropy via collective interactions
 - v_n quantify the event anisotropy
- Characterize key QGP properties like viscosity
 - Nearly perfect fluid: $1/4\pi < \eta/s < 3/4\pi$

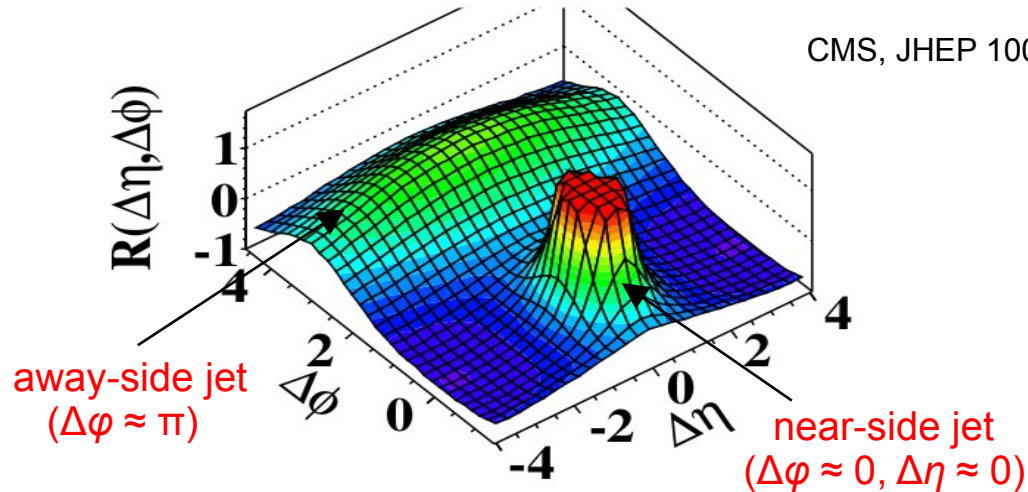
J. Bernhard et al., NP 19 (2019) 1113



Small collision systems: collectivity

(b) CMS MinBias, $1.0\text{GeV}/c < p_T < 3.0\text{GeV}/c$

CMS, JHEP 1009 (2010) 091

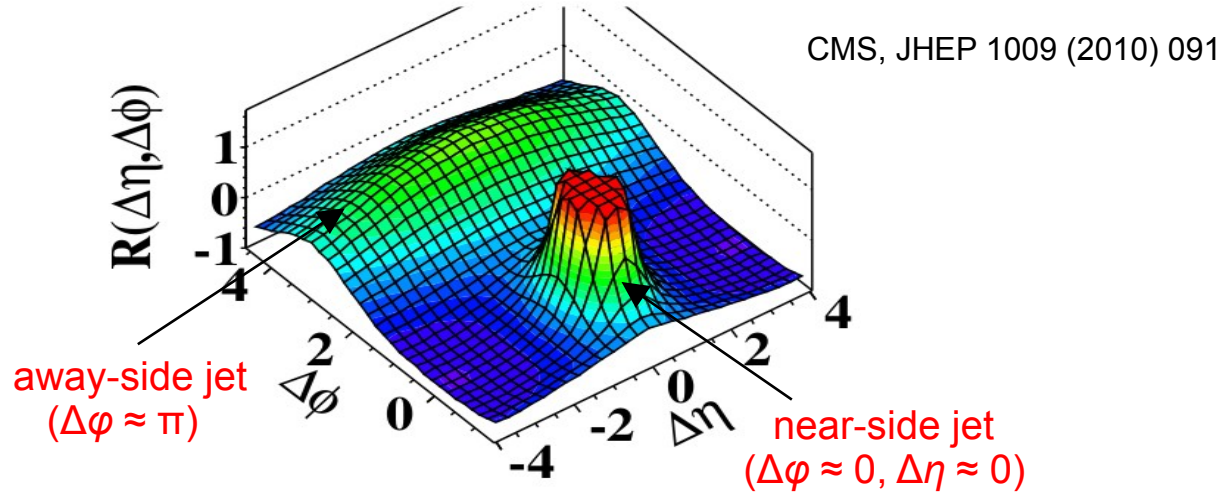


- Minimum bias pp
 - Nonflow contributions
 - Near-side jet peak (+resonances, HBT effects)
 - Recoil jet in away side

ALICE, PLB 719 (2012) 29
ATLAS, PRL 116 (2016) 172301

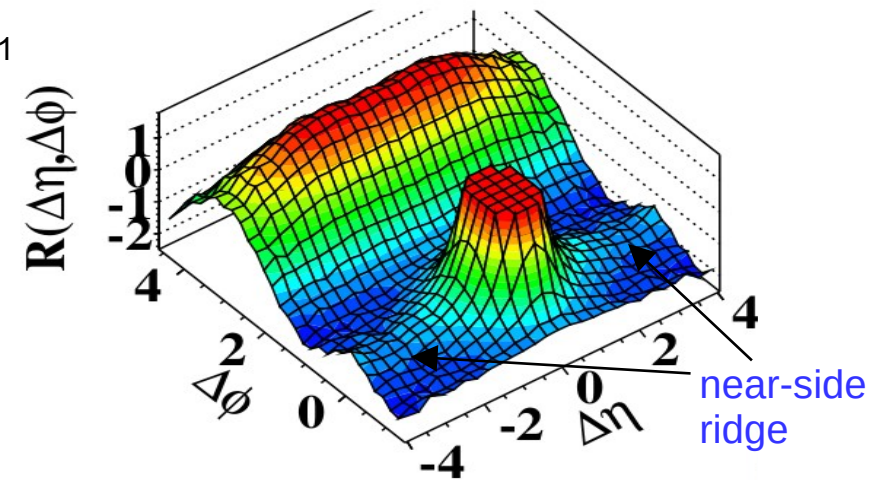
Small collision systems: collectivity

(b) CMS MinBias, $1.0\text{GeV}/c < p_T < 3.0\text{GeV}/c$



- Minimum bias pp
 - Nonflow contributions
 - Near-side jet peak (+resonances, HBT effects)
 - Recoil jet in away side

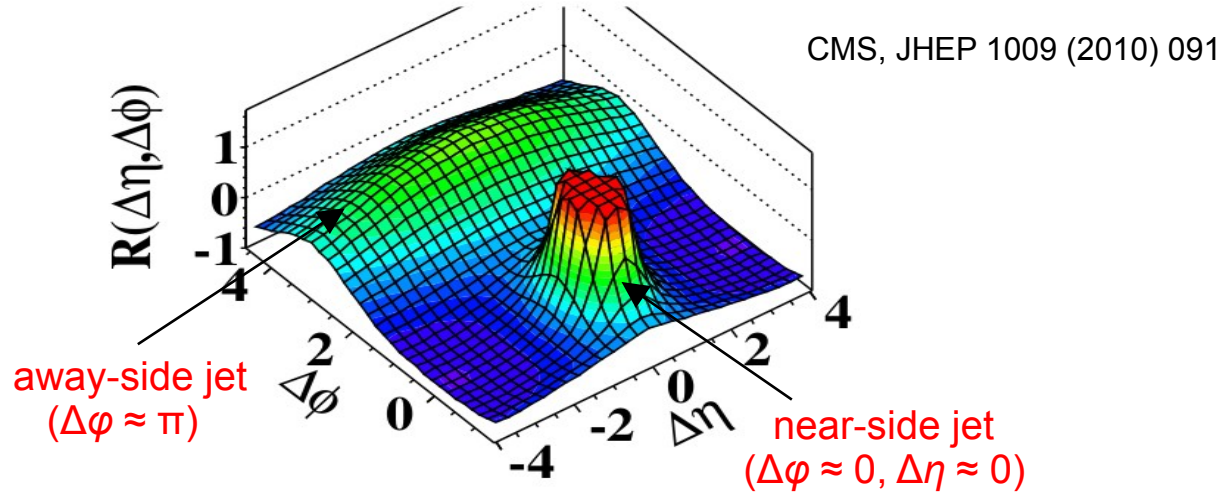
(d) CMS $N \geq 110$, $1.0\text{GeV}/c < p_T < 3.0\text{GeV}/c$



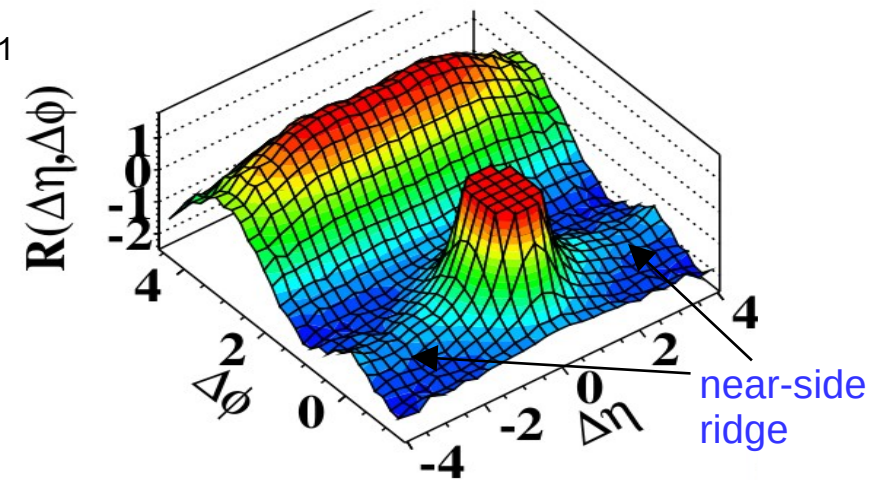
- High multiplicity pp
 - Near-side ridge, typical of collective systems
 - Decomposed into Fourier harmonics

Small collision systems: collectivity

(b) CMS MinBias, $1.0\text{GeV}/c < p_T < 3.0\text{GeV}/c$



(d) CMS $N \geq 110$, $1.0\text{GeV}/c < p_T < 3.0\text{GeV}/c$



- Minimum bias pp

- Nonflow contributions

- Near-side jet peak (+resonances, HBT effects)
 - Recoil jet in away side

- High multiplicity pp

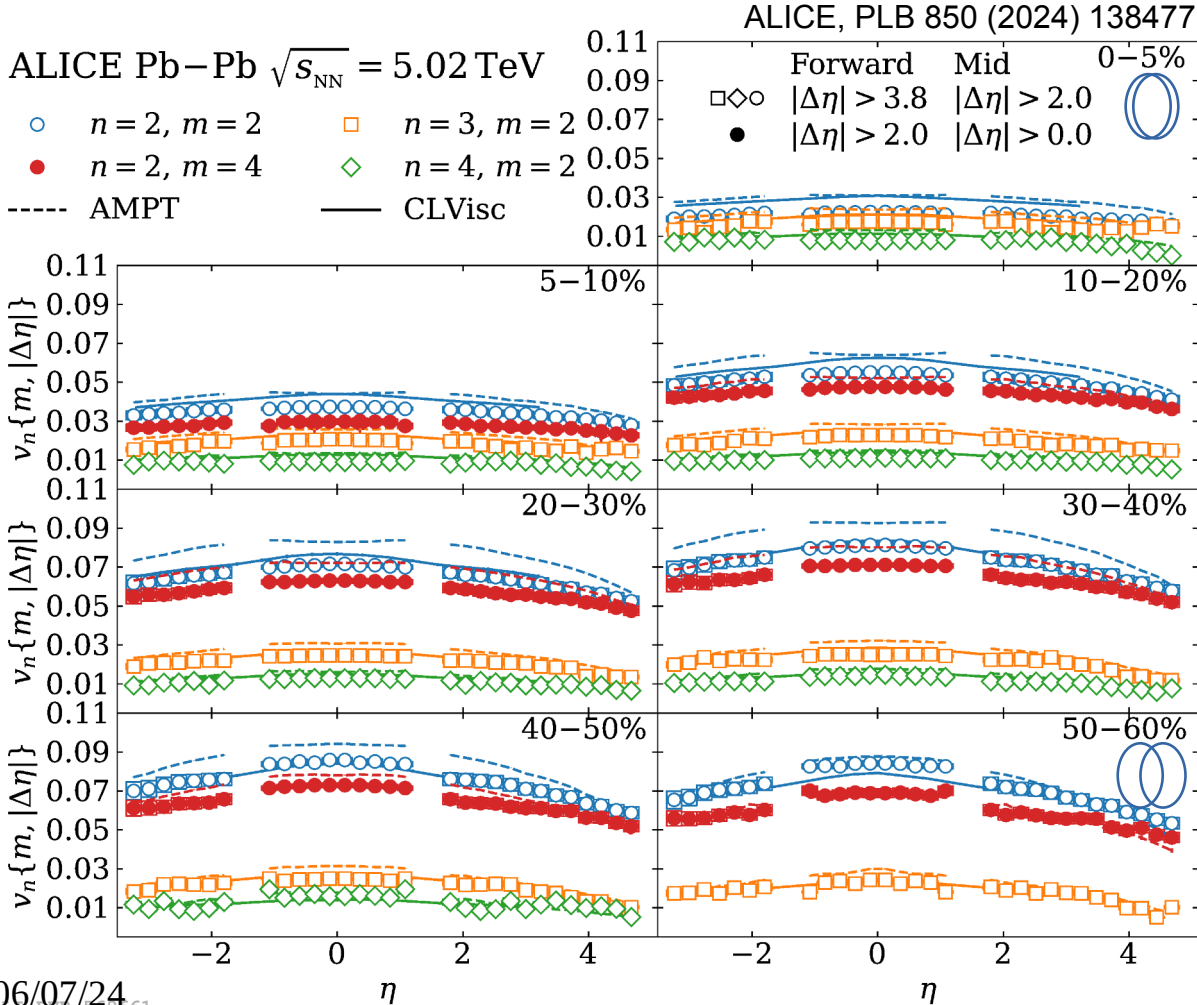
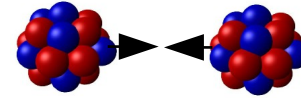
- Near-side ridge, typical of collective systems
 - Decomposed into Fourier harmonics

ALICE, PLB 719 (2012) 29
ATLAS, PRL 116 (2016) 172301

What is the origin of these collective effects?

Collectivity

Anisotropic flow at forward rapidity

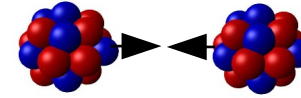
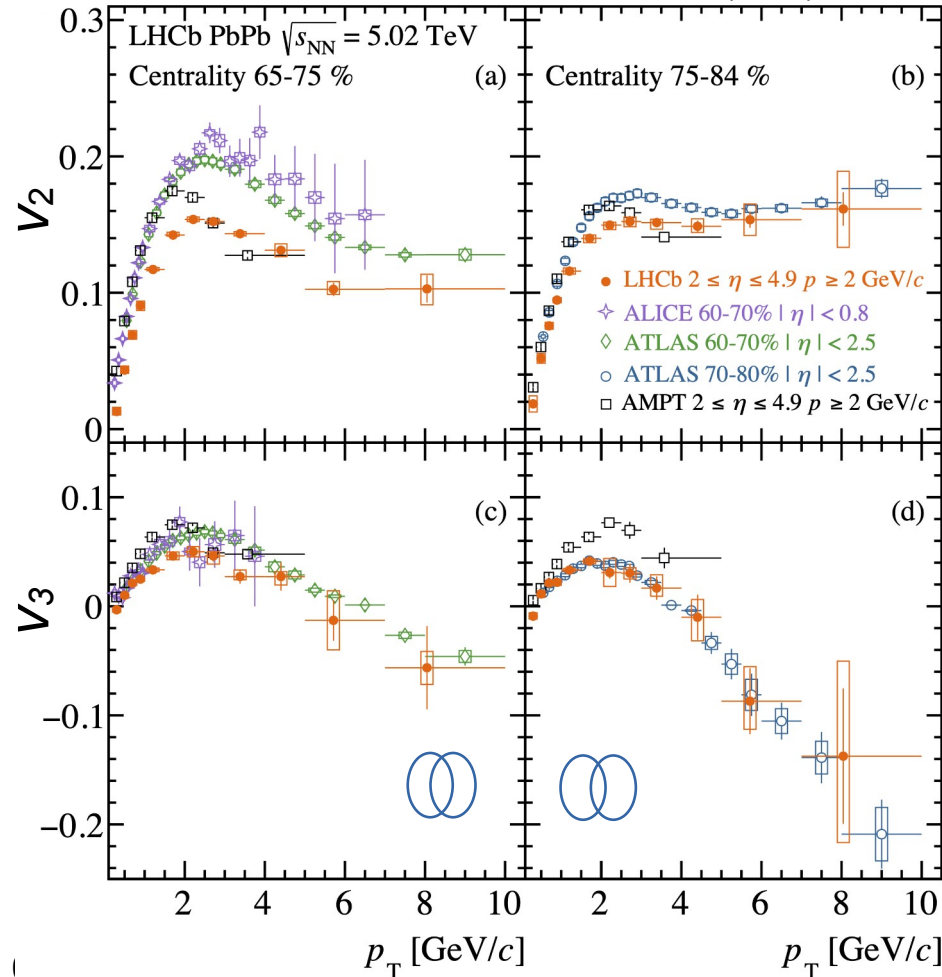


- Measurements of v_2 , v_3 , and v_4 coefficients are extended at large η
 - Hit-based analysis
- v_2 shows strong centrality dependence
- v_3 and v_4 reveal a modest centrality dependence
- Models overestimate the measured v_n coefficients
 - Constrain initial conditions

$$\frac{dN}{d\varphi} \sim 1 + \sum_{n=1}^{\infty} 2v_n \cos(n(\varphi - \Psi_n))$$

Anisotropic flow at forward rapidity

LHCb, PRC 109 (2024) 054908

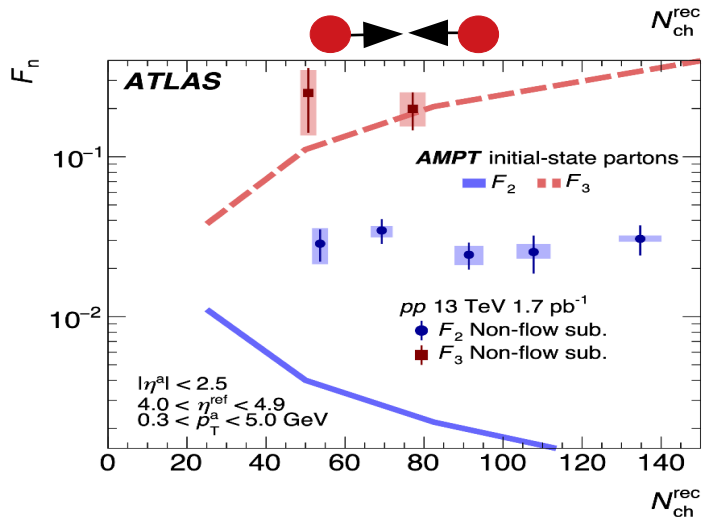
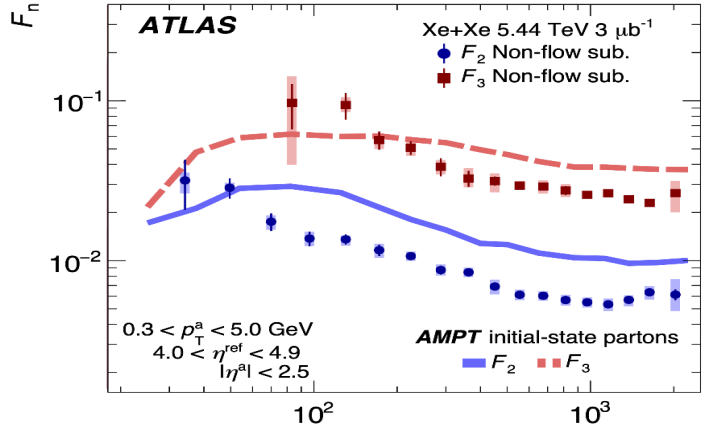


- Measurements of $v_2(p_T)$ and $v_3(p_T)$ coefficients at forward rapidity
 - Similar trends but different magnitudes than reported at central rapidity
 - Pseudorapidity range, nonflow contributions
 - Constrain models

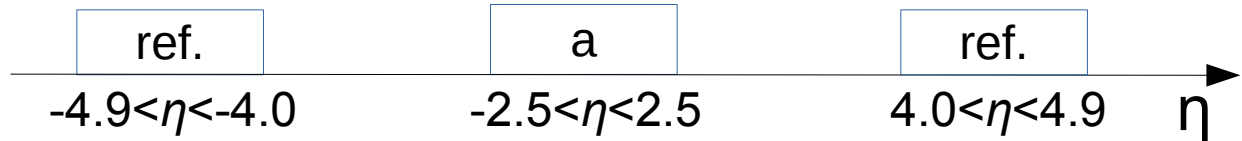
Longitudinal flow decorrelations



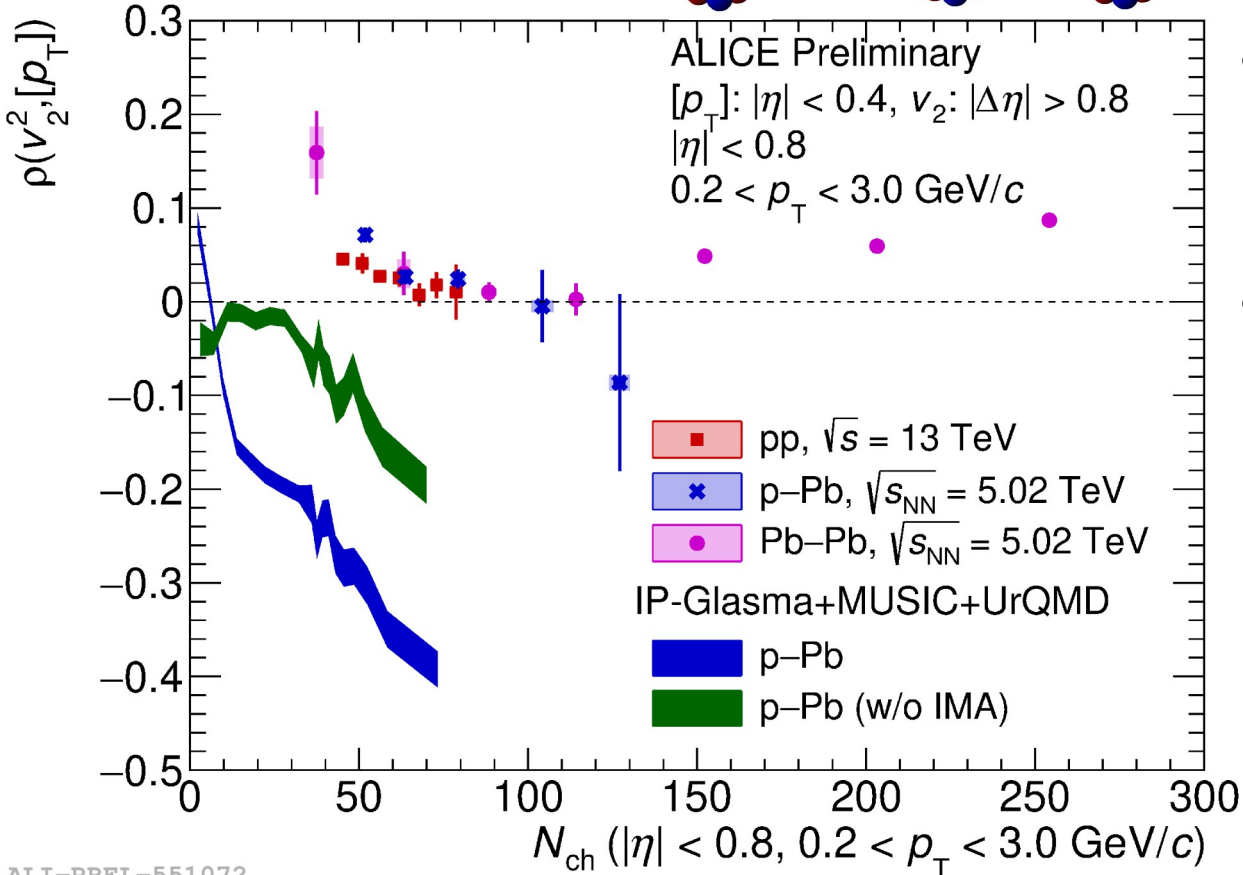
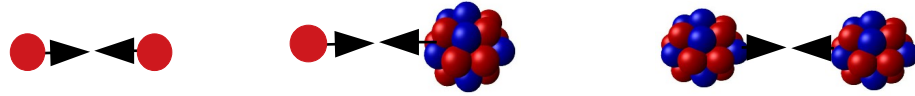
ATLAS, arXiv:2308.16745



- Constrain geometry in longitudinal direction
 - Measure 2-particle correlations between two η regions
 - Parametrize with $c_n = A_n(1 + F_n\eta + S_n\eta^2)$
 - F_n characterize the linear decorrelation strength
- Comparison with model with no geometric decorrelation
 - Qualitatively agreement in Xe–Xe but not in pp collisions
 - Evidence for longitudinal fluctuations in pp collisions possibly from subnucleonic structures



v_2^2 - $[p_T]$ correlations



- Probe the initial stage
 - $\rho < 0$: geometric response
 - $\rho > 0$: Color Glass Condensate (CGC)
- Decreasing trend with increasing multiplicity in pp and p-Pb collisions
 - Not explained by simple geometry picture
 - Not described by a CGC-based hybrid model (w/wo initial momentum anisotropy)

$$\rho(v_n^2, [p_T]) = \frac{\text{Cov}(v_n^2, [p_T])}{\sqrt{\text{Var}(v_n^2)} \sqrt{c_k}}$$

Ridge yields

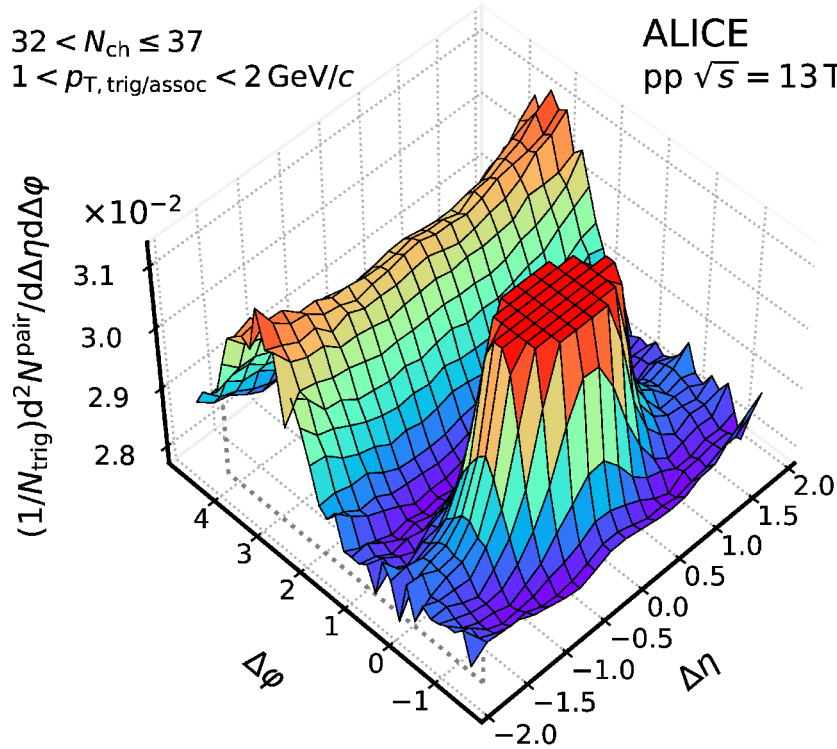


ALICE, PRL 132 (2024) 172302



$32 < N_{ch} \leq 37$
 $1 < p_{T, \text{trig/assoc}} < 2 \text{ GeV}/c$

ALICE
 $pp \sqrt{s} = 13 \text{ TeV}$



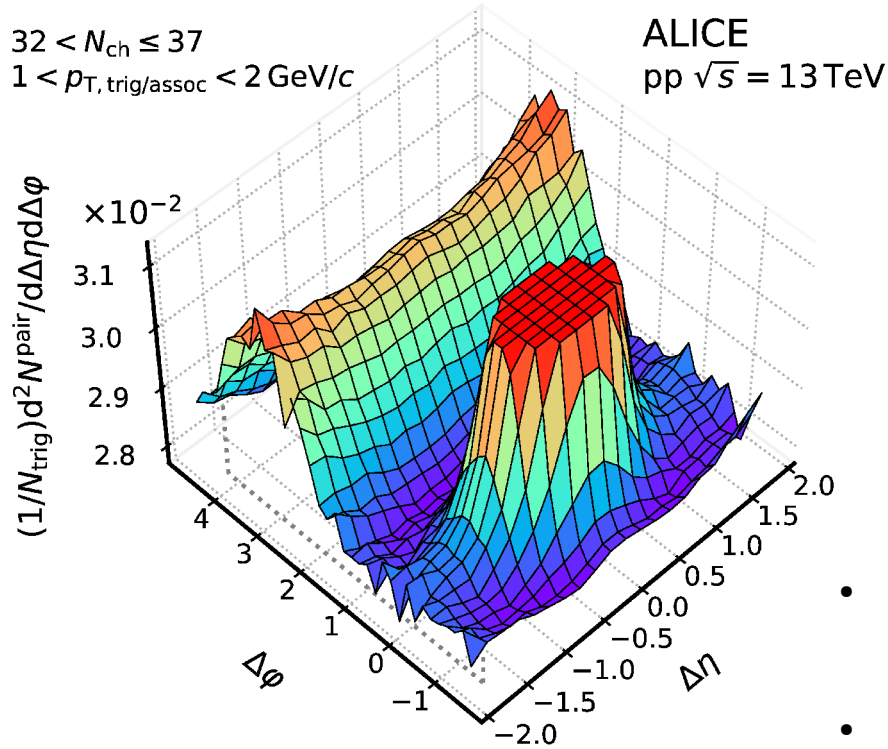
- Ridge yields to study collective effects down to low multiplicities
 - Overlap with e^+e^- results from ALEPH at $\sqrt{s} = 91 \text{ GeV}$

ALI-PUB-566419

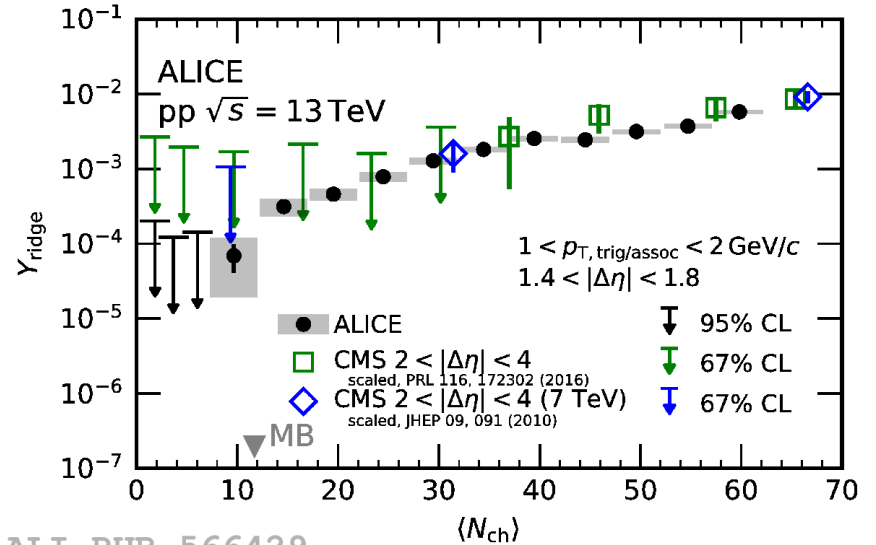
Ridge yields



ALICE, PRL 132 (2024) 172302



ALI-PUB-566419



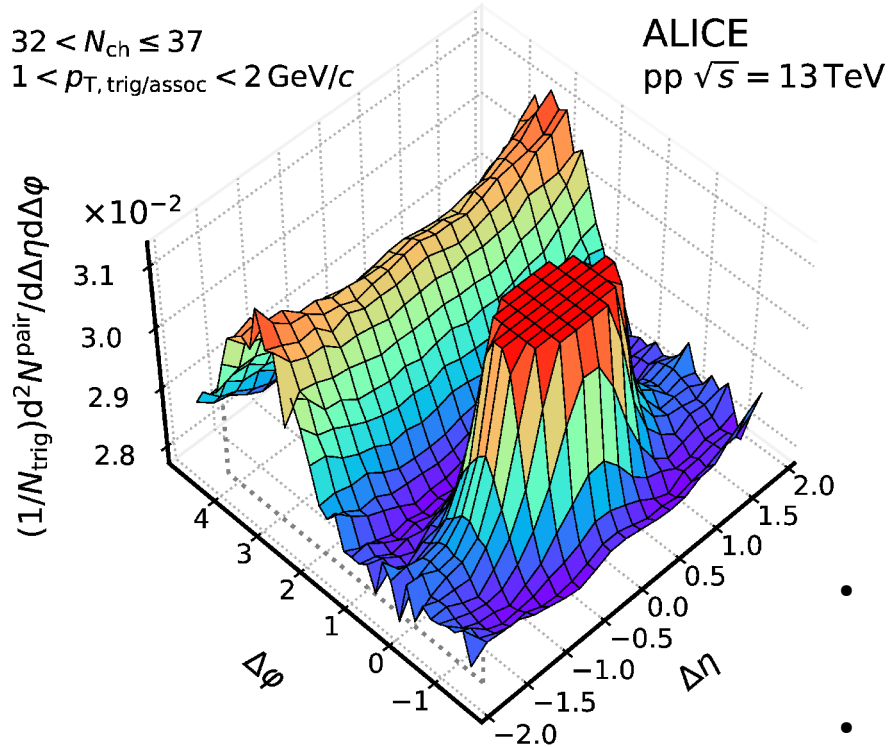
ALI-PUB-566429

- Ridge yields to study collective effects down to low multiplicities
 - Overlap with e^+e^- results from ALEPH at $\sqrt{s} = 91 \text{ GeV}$
- Strong multiplicity dependence
 - Good agreement with CMS results

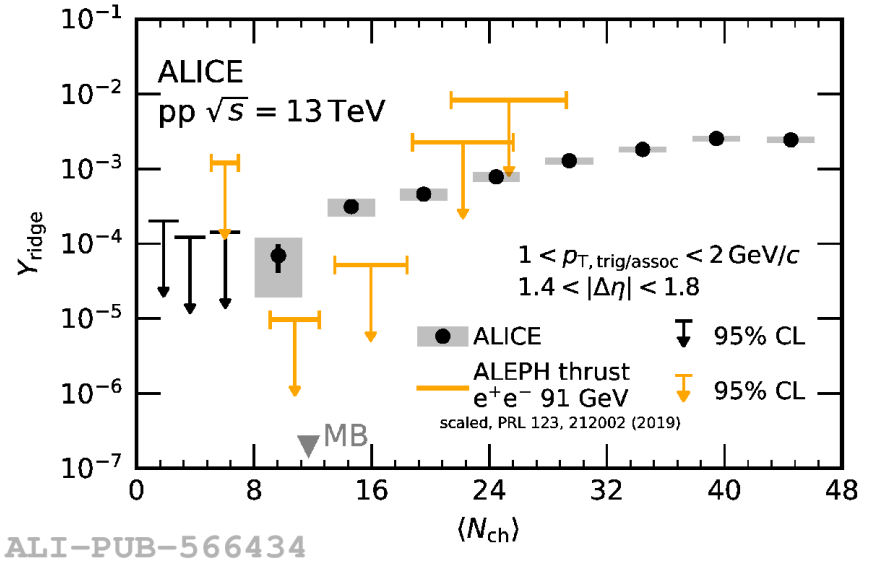
Ridge yields



ALICE, PRL 132 (2024) 172302



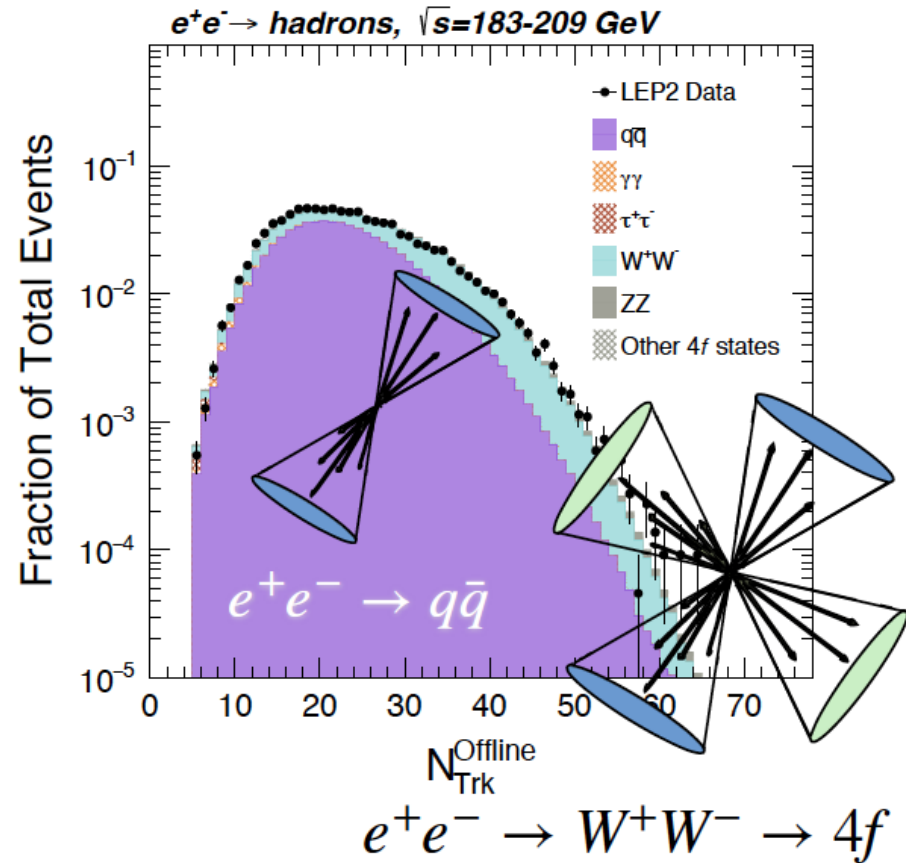
ALI-PUB-566419



- Ridge yields to study collective effects down to low multiplicities
 - Overlap with e^+e^- results from ALEPH at $\sqrt{s} = 91 \text{ GeV}$
- Strong multiplicity dependence
 - Good agreement with CMS results
 - Large differences between pp and e^+e^- results for $N_{ch} < 18$

Ridge yields

Y-C. Chen *et al.*, arXiv: 2312.05084

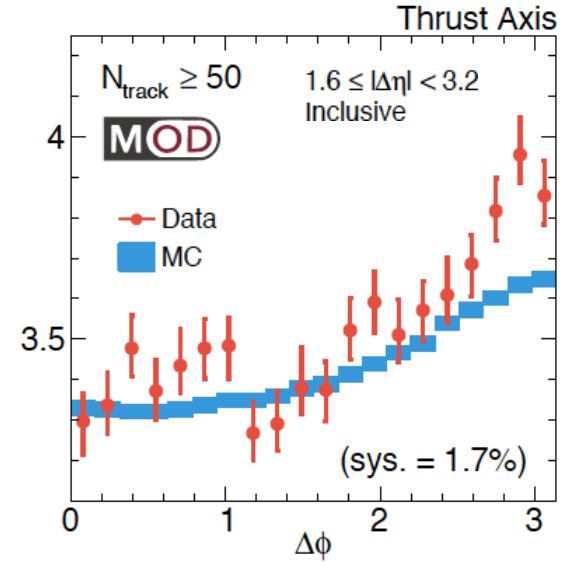
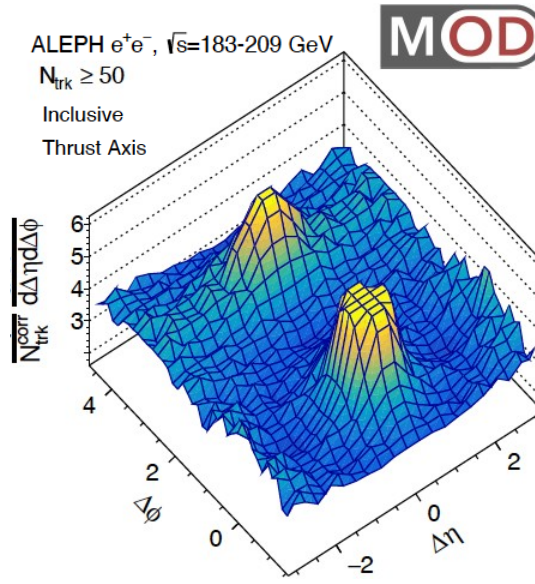
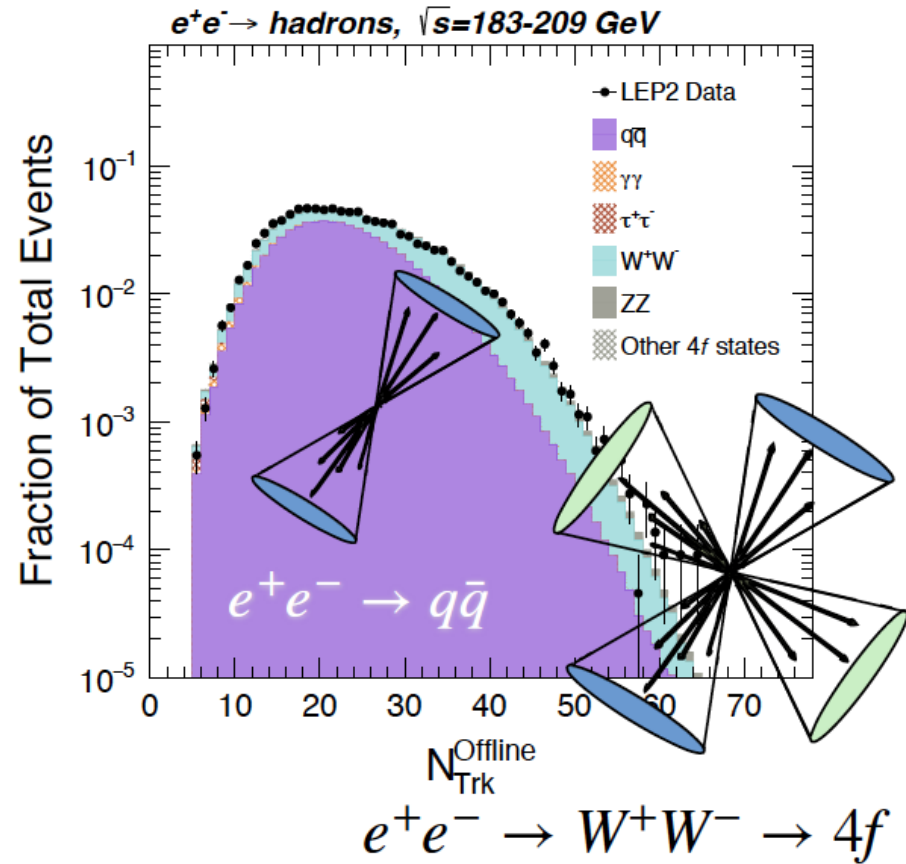


- 2-particle correlations on LEP-II e^+e^- data

Ridge yields



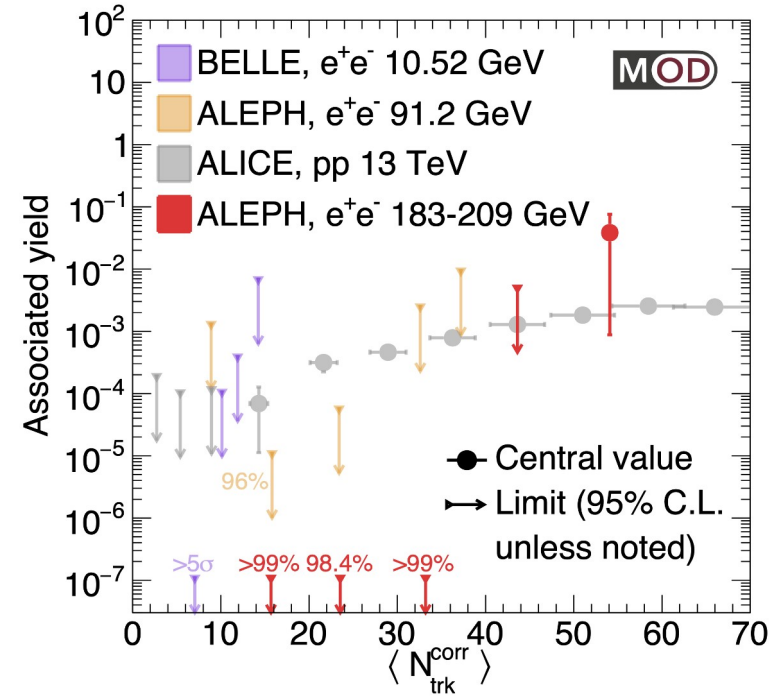
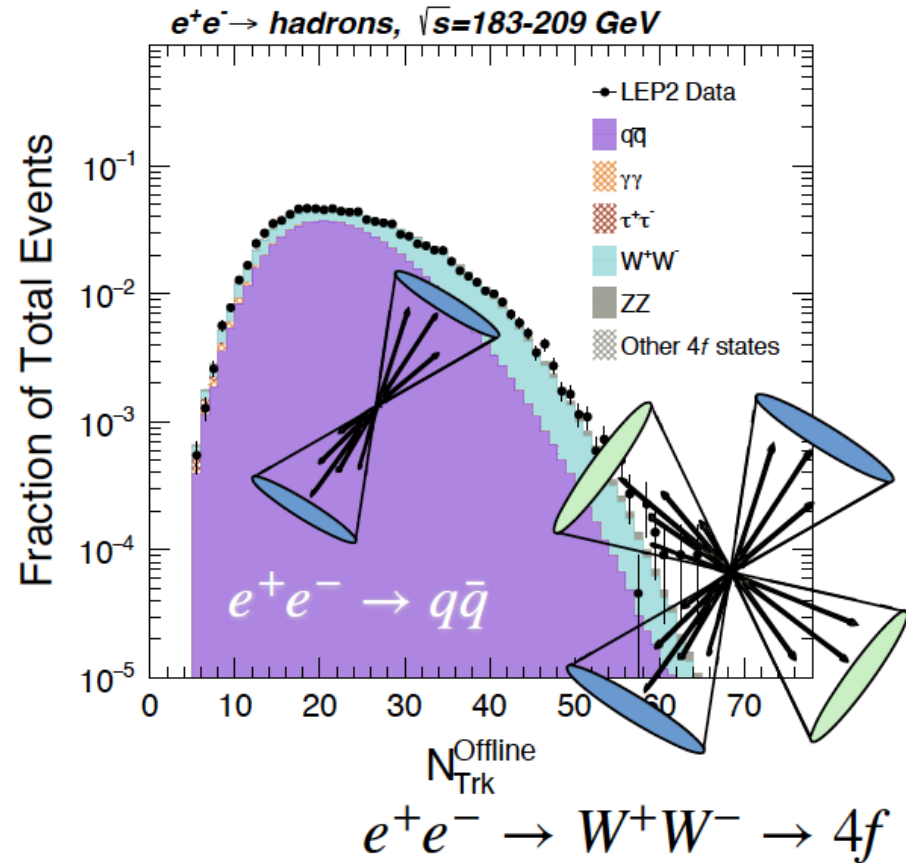
Y.-C. Chen *et al.*, arXiv: 2312.05084



- 2-particle correlations on LEP-II e^+e^- data
- High multiplicity: excess of azimuthal anisotropy signals
 - Long-range near-side structure
 - Narrow away-side structure

Ridge yields

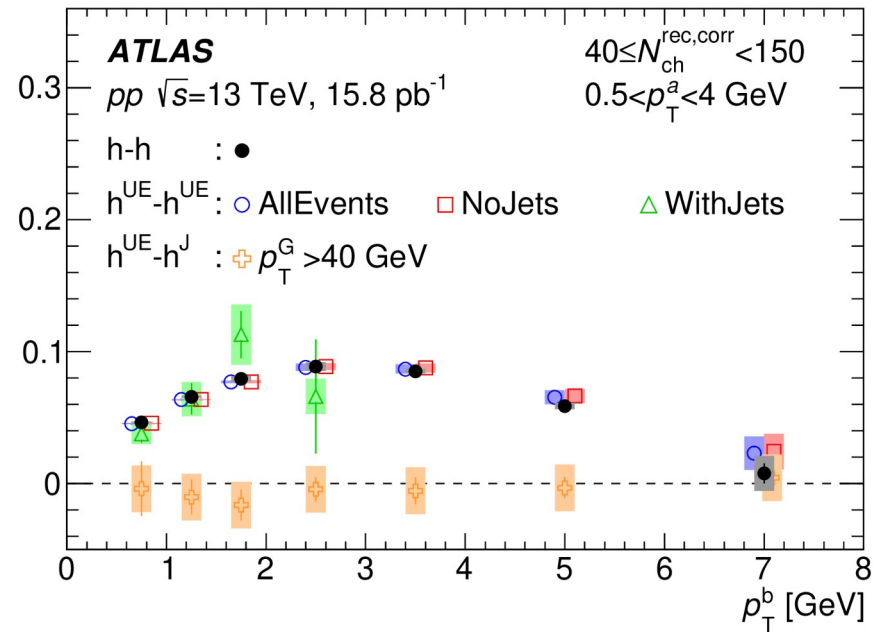
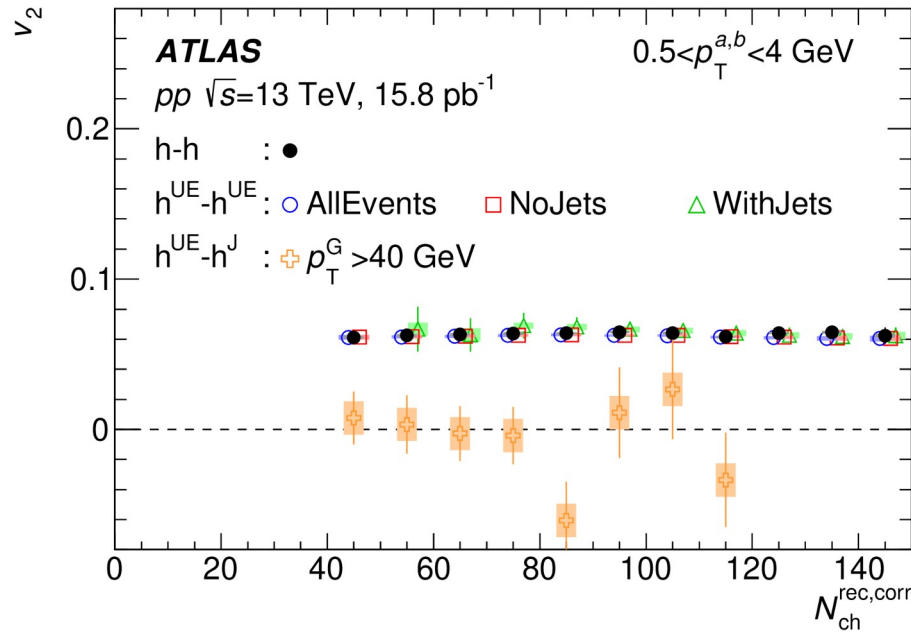
Y.-C. Chen *et al.*, arXiv: 2312.05084



- 2-particle correlations on LEP-II e^+e^- data
- High multiplicity: excess of azimuthal anisotropy signals
 - Long-range near-side structure
 - Narrow away-side structure
- No ridge signals in e^+e^- for $N_{\text{ch}} < 40$

v_2 w/wo jets

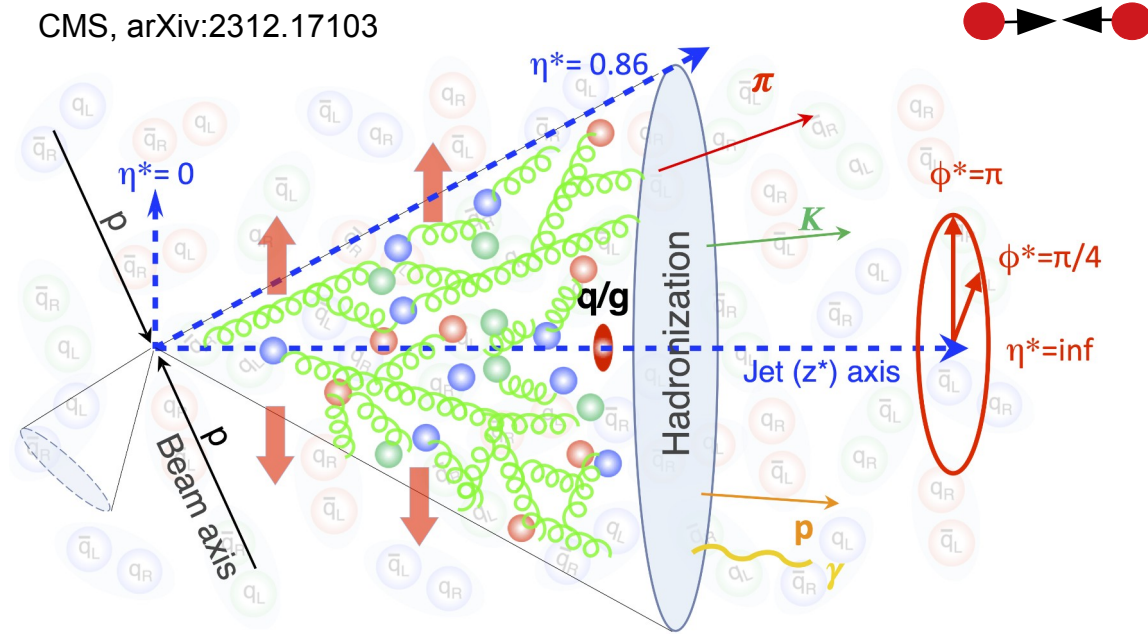
ATLAS, PRL 131 (2023) 162301



- Check if ridge is associated with jet production
 - 2-particle correlations for particles from UE or associated with jets
- No dependence on jets presence for v_2
- $v_2 \sim 0$ for UE–jet particles correlations

In-jet v_2

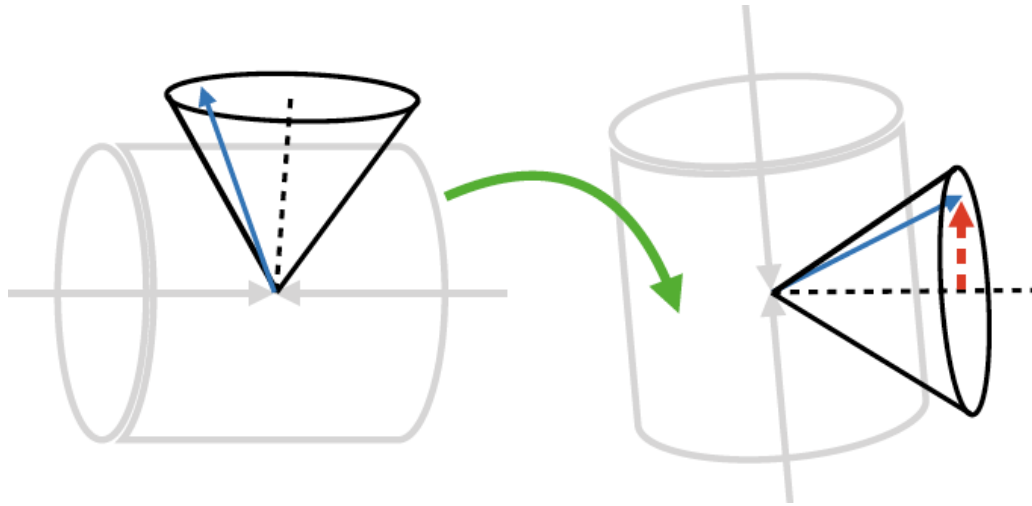
CMS, arXiv:2312.17103



- Search for v_2 in individual jets

In-jet v_2

CMS, arXiv:2312.17103



- Search for v_2 in individual jets
- 2-particle correlations in rotated frame

CMS

138 fb⁻¹ (pp 13 TeV)

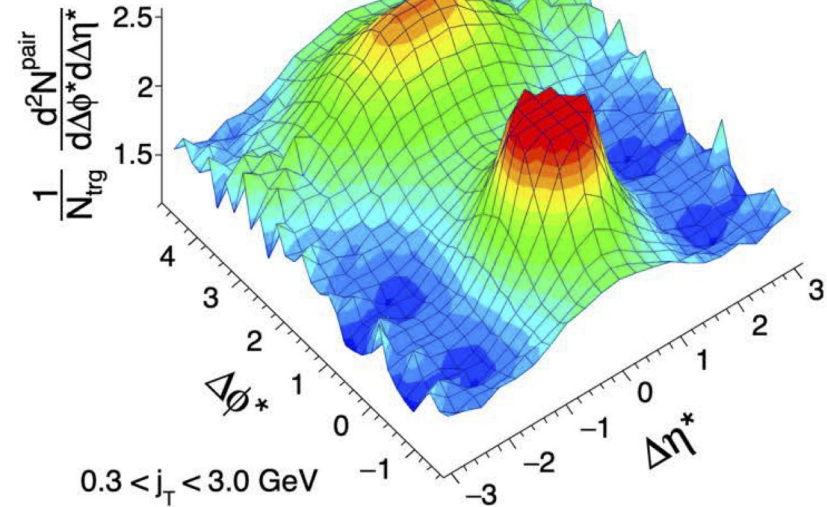
$\langle N_{ch}^j \rangle = 101$

Top 0.0023% highest- N_{ch}^j jets

Anti k_T R=0.8

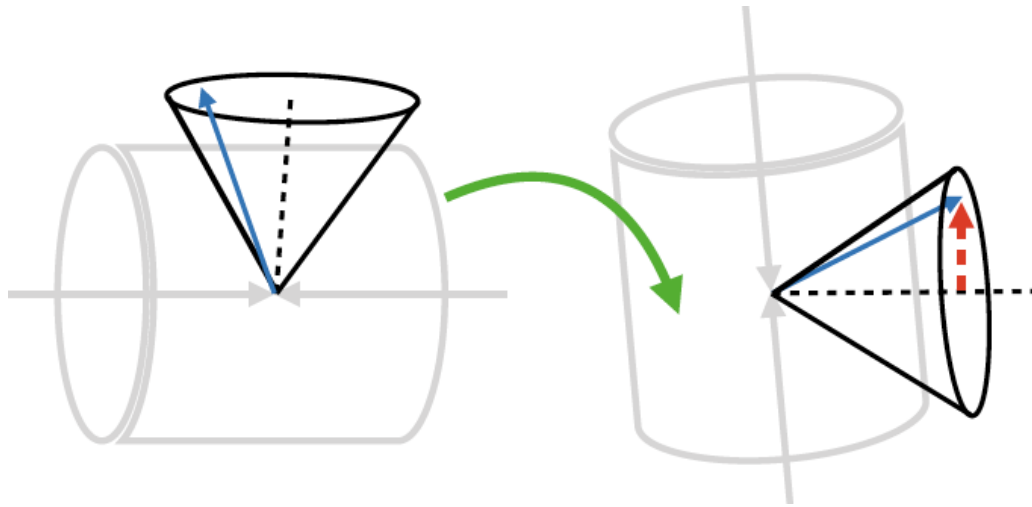
$p_T^{\text{jet}} > 550$

$|\eta^{\text{jet}}| < 1.6$

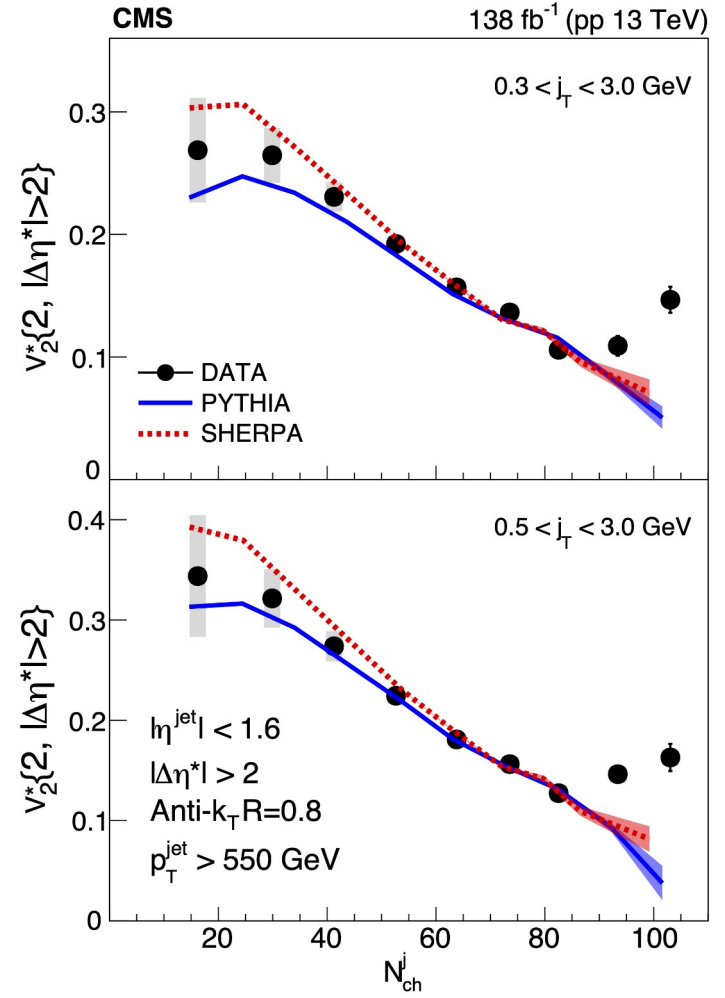


In-jet v_2

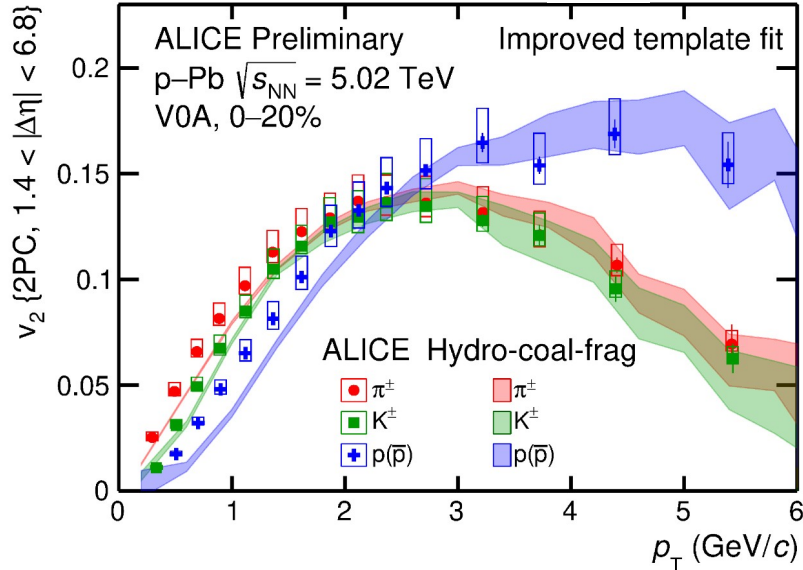
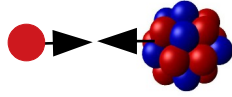
CMS, arXiv:2312.17103



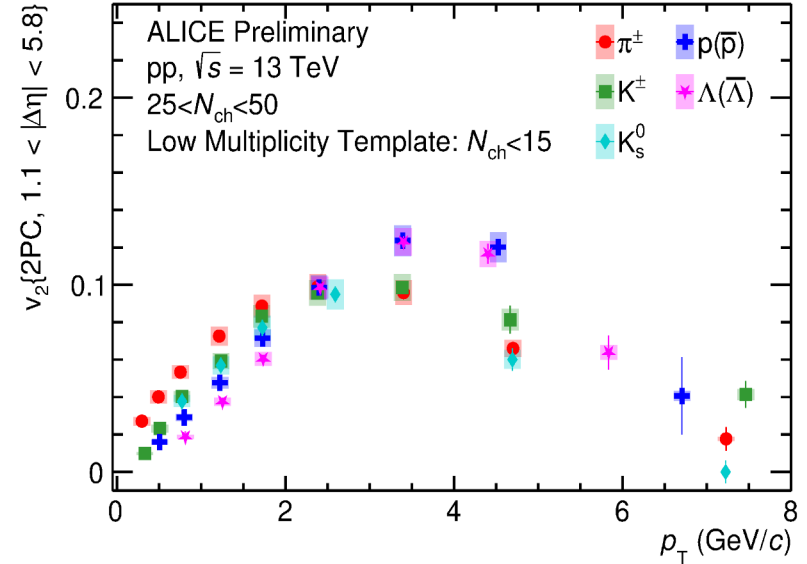
- Search for v_2 in individual jets
- 2-particle correlations in rotated frame
- $N_{ch}^{jet} < 80$: good agreement with MC
- $N_{ch}^{jet} > 80$: upward trend \rightarrow collectivity in jets?



v_2 of identified particles



ALI-PREL-503282

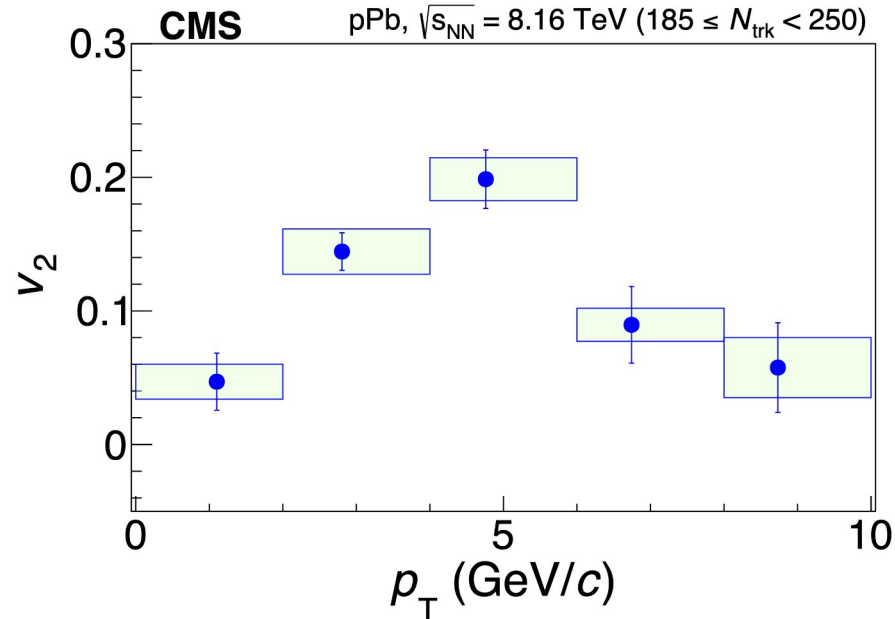
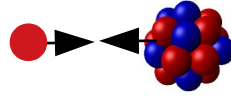


ALI-PREL-573050

- Low p_T : consistent with mass ordering
- Intermediate p_T : particle type grouping
- Described by hydrodynamics with coalescence and jet fragmentation
 - No jet quenching yet!

v_2 of $f_0(980)$

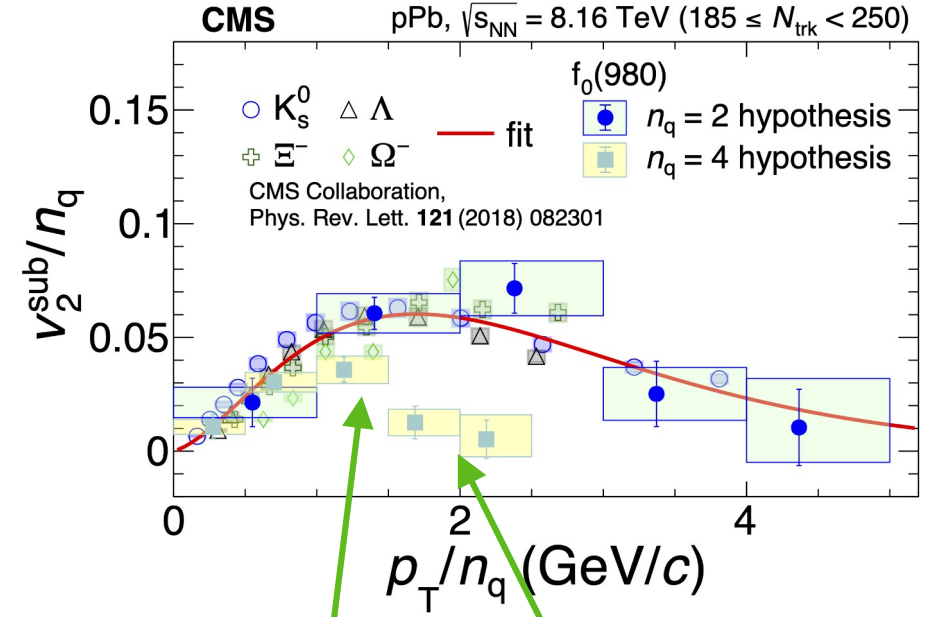
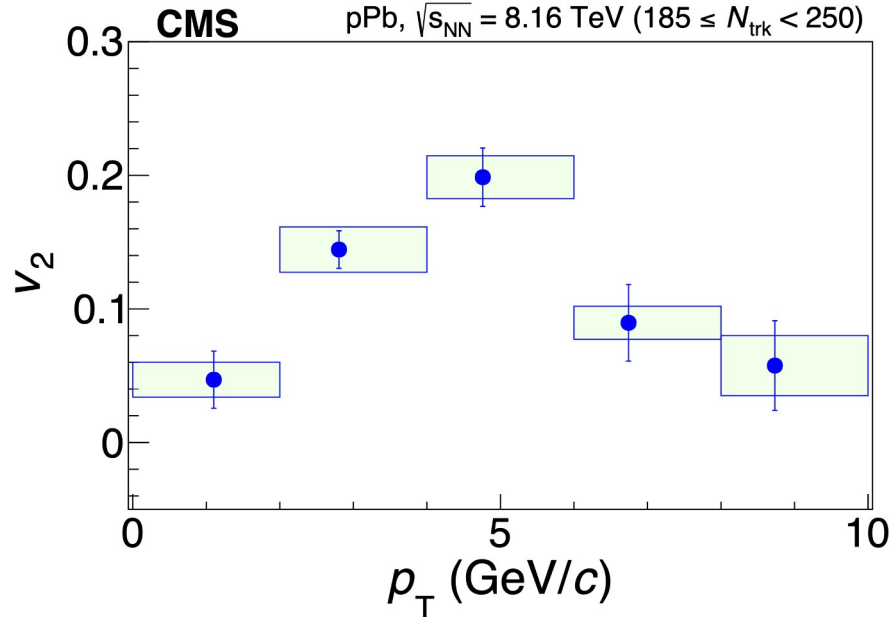
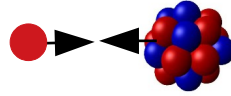
CMS, arXiv:2312.17092



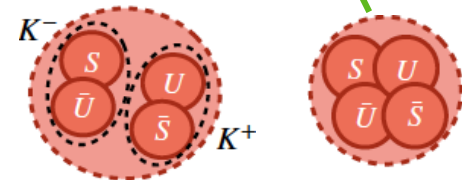
- Structure unknown: diquark, tetraquark, KK molecule
Use v_2/n_q scaling to extract number of quarks

v_2 of $f_0(980)$

CMS, arXiv:2312.17092

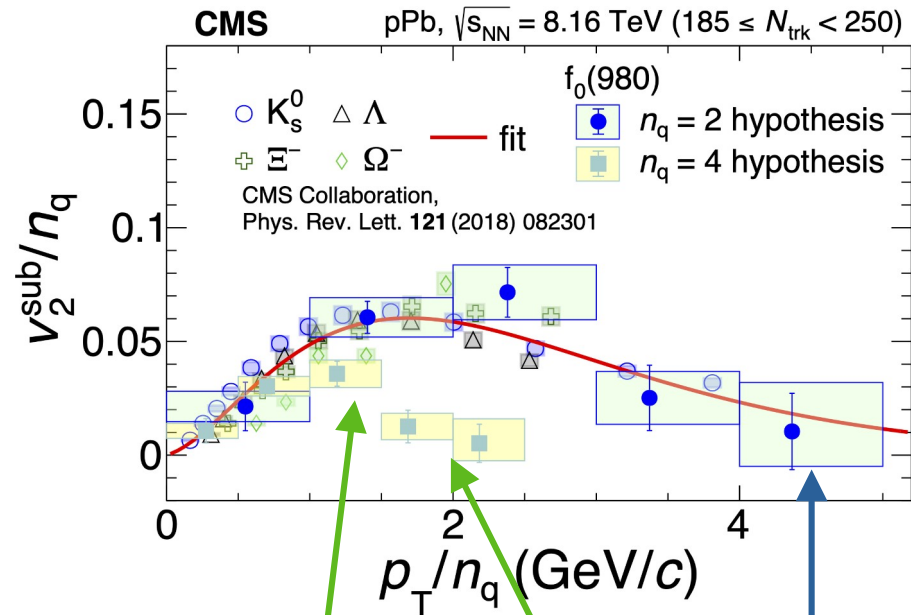
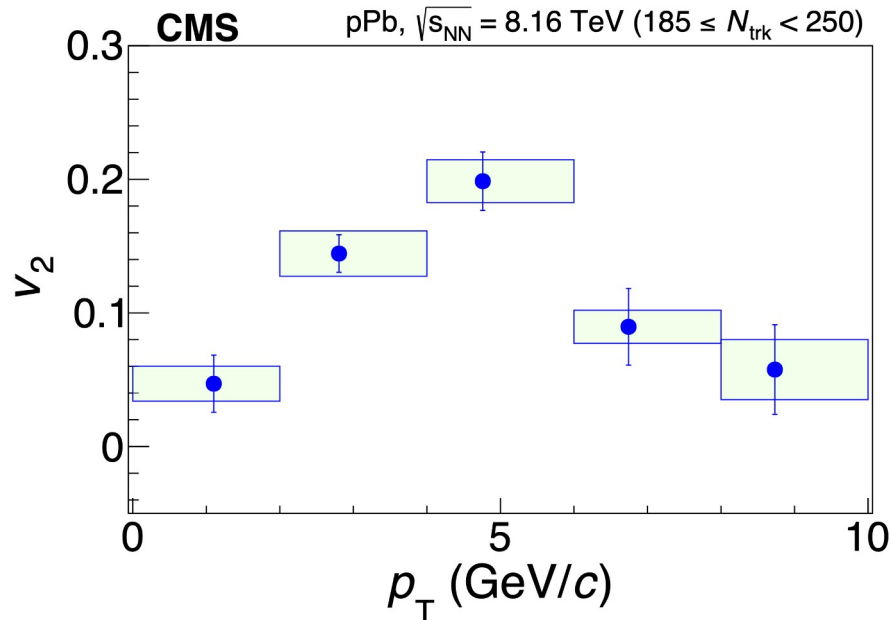
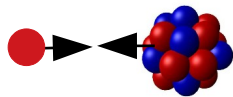


- Structure unknown: diquark, tetraquark, KK molecule
 - Use v_2/n_q scaling to extract number of quarks
- $n_q = 4$ excluded at $\geq 3.1\sigma$

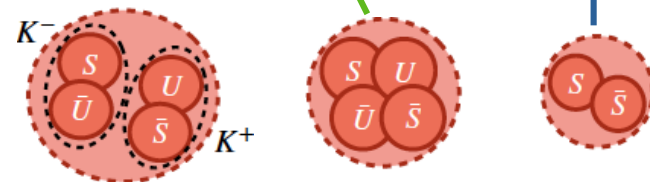


v_2 of $f_0(980)$

CMS, arXiv:2312.17092

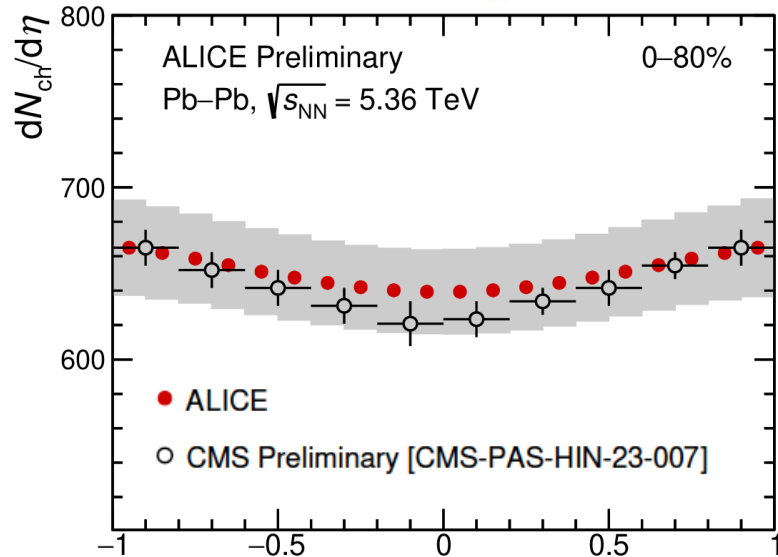
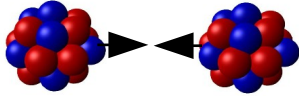


- Structure unknown: diquark, tetraquark, KK molecule
 - Use v_2/n_q scaling to extract number of quarks
- $n_q = 4$ excluded at $\geq 3.1\sigma$
- $n_q = 2$ favored



Particle production

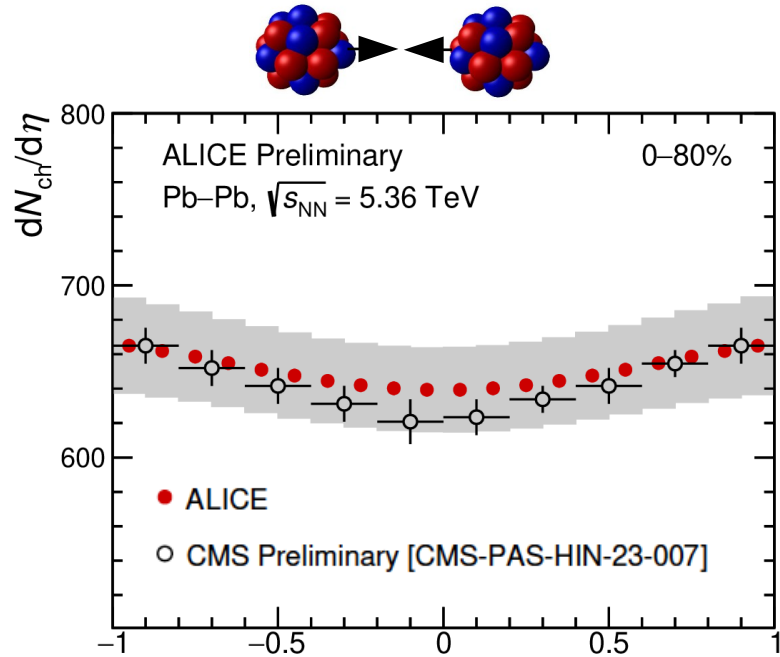
$dN_{\text{ch}}/d\eta$ in Run 3



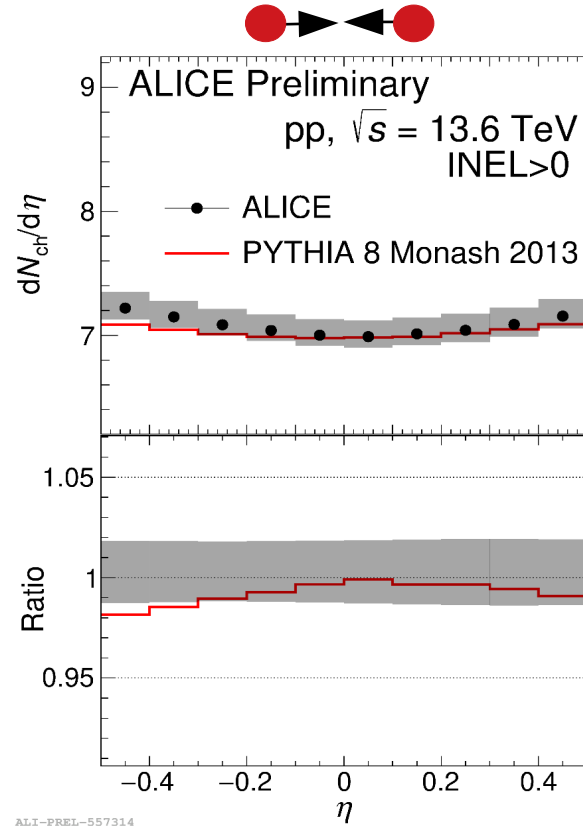
ALI-PREL-571640

- $dN_{\text{ch}}/d\eta$ measured at highest energy in Pb-Pb

$dN_{ch}/d\eta$ in Run 3



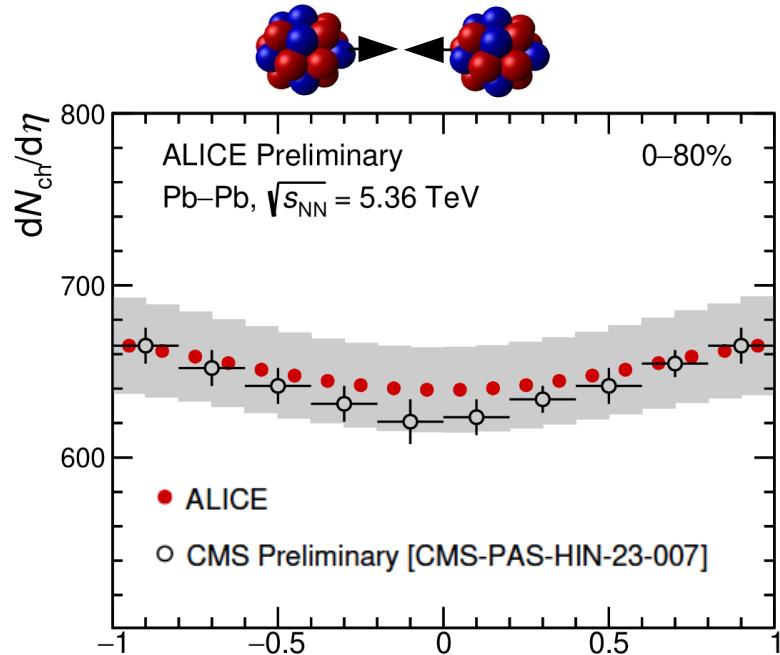
ALI-PREL-571640



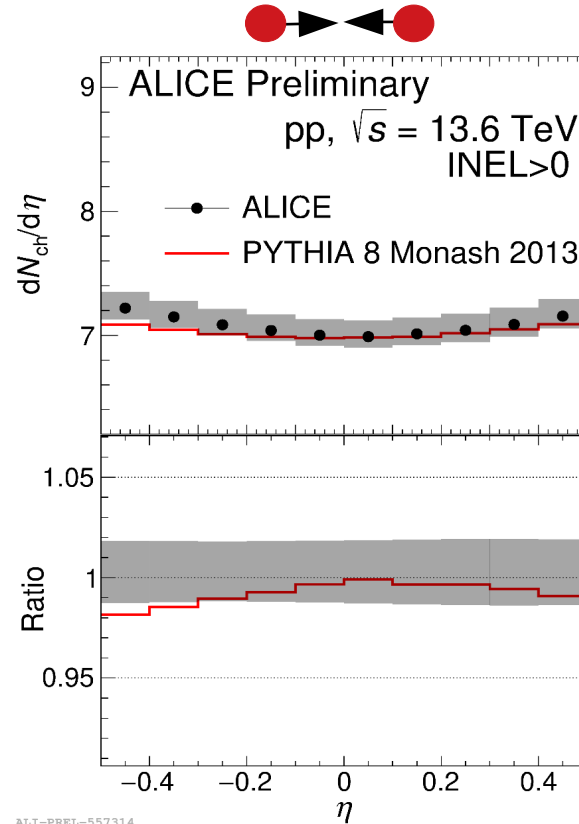
ALI-PREL-557314

- $dN_{ch}/d\eta$ measured at highest energy in Pb-Pb and pp collisions

$dN_{ch}/d\eta$ in Run 3



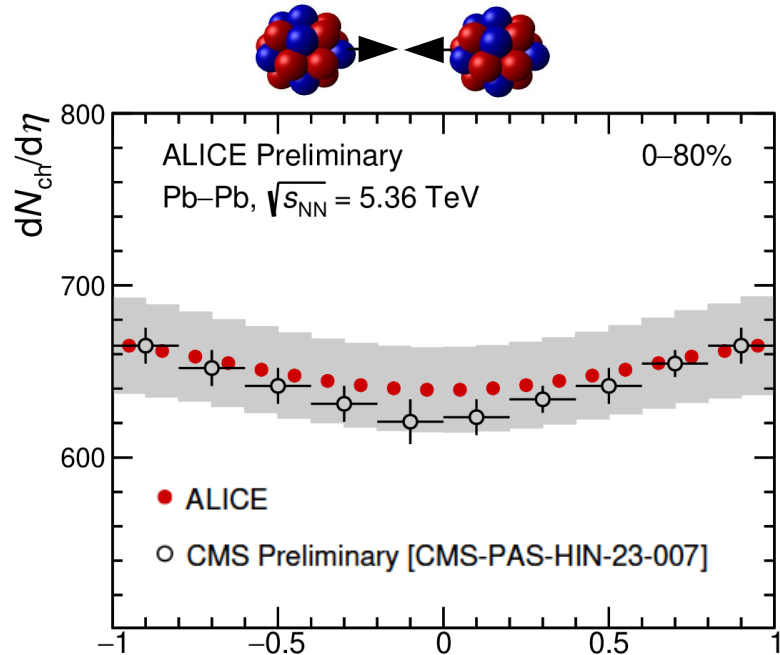
ALI-PREL-571640



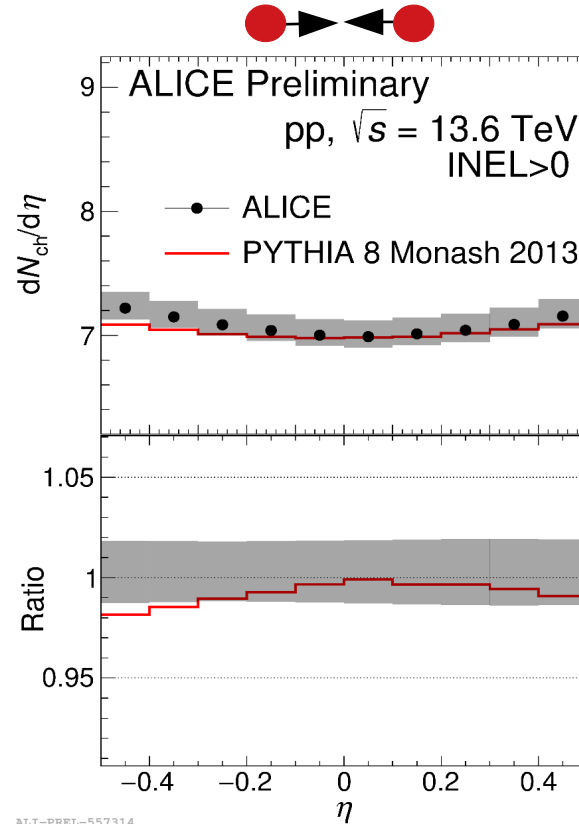
ALI-PREL-557314

- $dN_{ch}/d\eta$ measured at highest energy in Pb-Pb and pp collisions
- Magnitude and shape not fully described by MC calculations

$dN_{ch}/d\eta$ in Run 3



ALI-PREL-571640

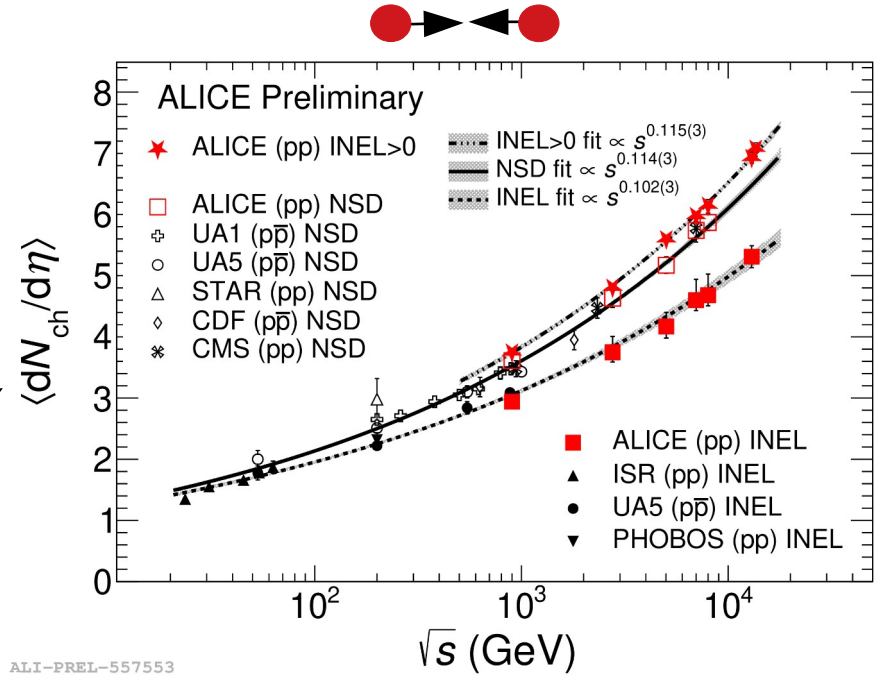
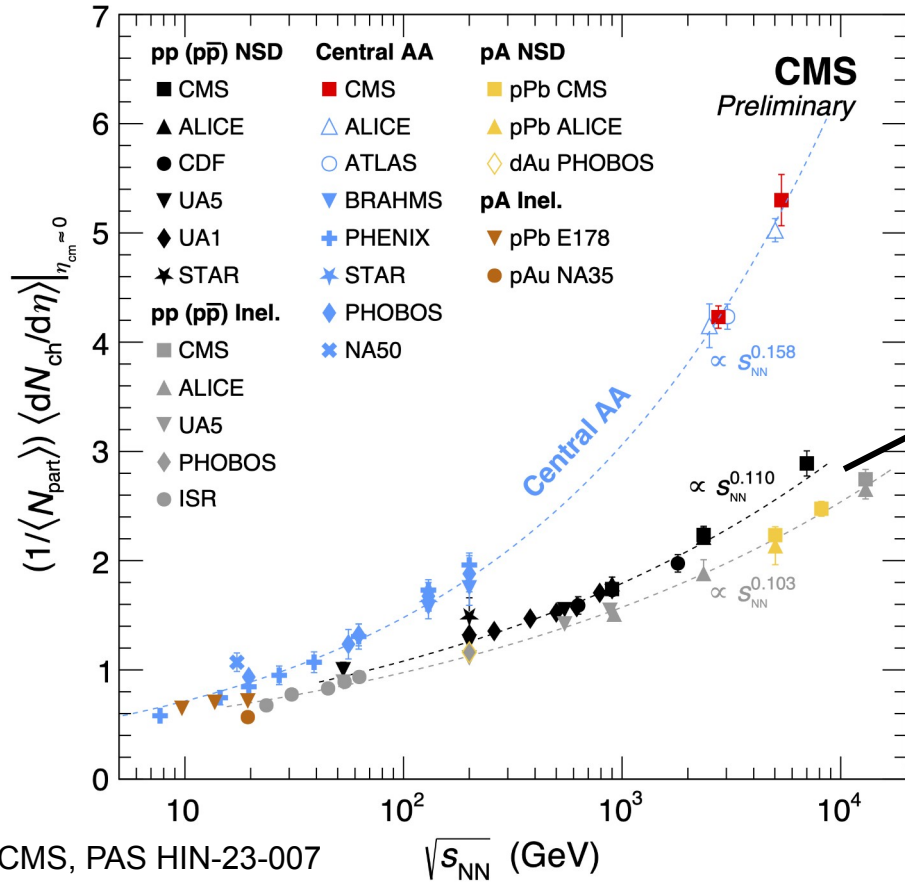


ALI-PREL-557314

- $dN_{ch}/d\eta$ measured at highest energy in Pb–Pb and pp collisions
- Magnitude and shape not fully described by MC calculations

- Constrain initial conditions and evolution of AA collisions
- Constrain gluon saturation effects and nuclear shadowing

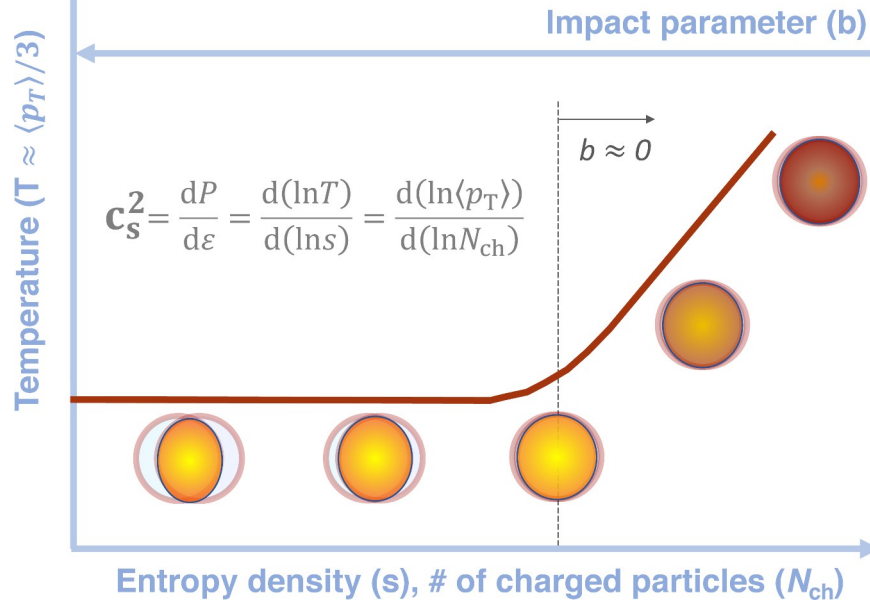
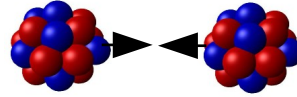
$dN_{ch}/d\eta$ in Run 3



- $\sqrt{s_{NN}}$ dependence consistent with power law from lower energies
 - Grows faster in AA than in pp collisions

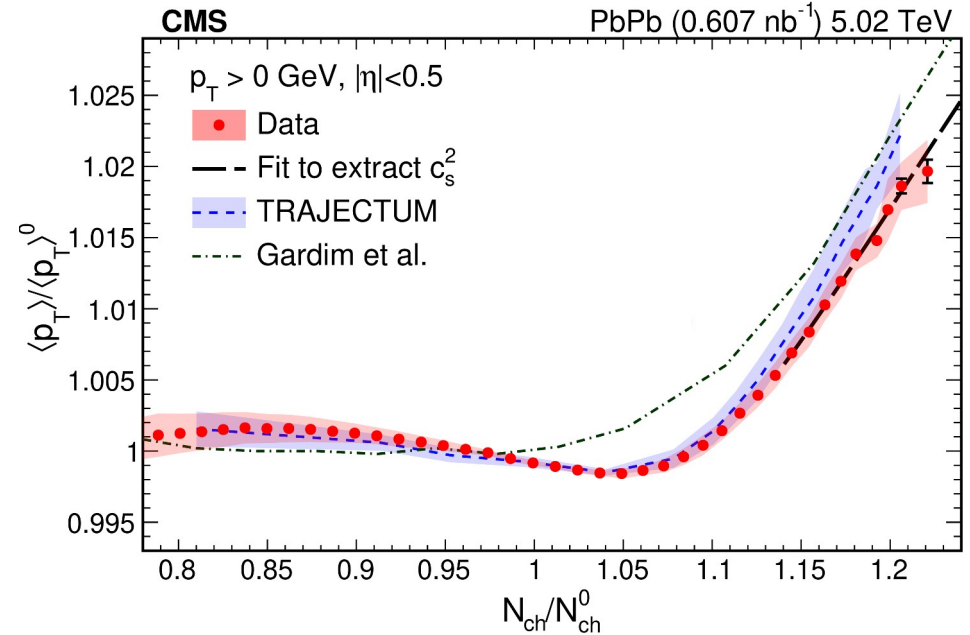
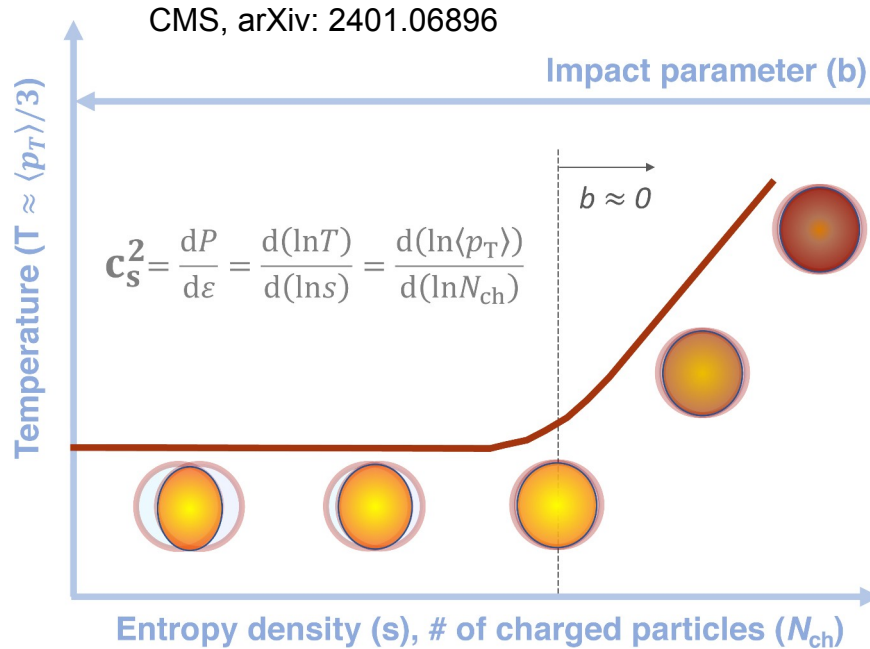
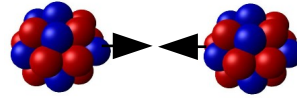
Speed of sound in QGP

CMS, arXiv: 2401.06896



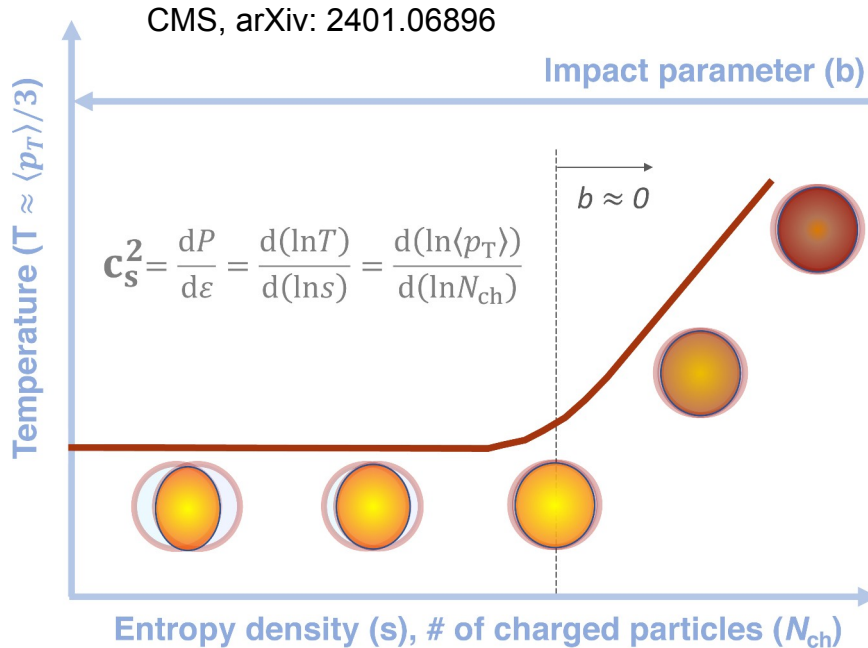
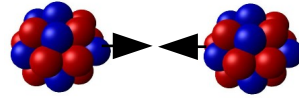
- c_s^2 can be extracted from $\langle p_T \rangle$ and N_{ch}

Speed of sound in QGP

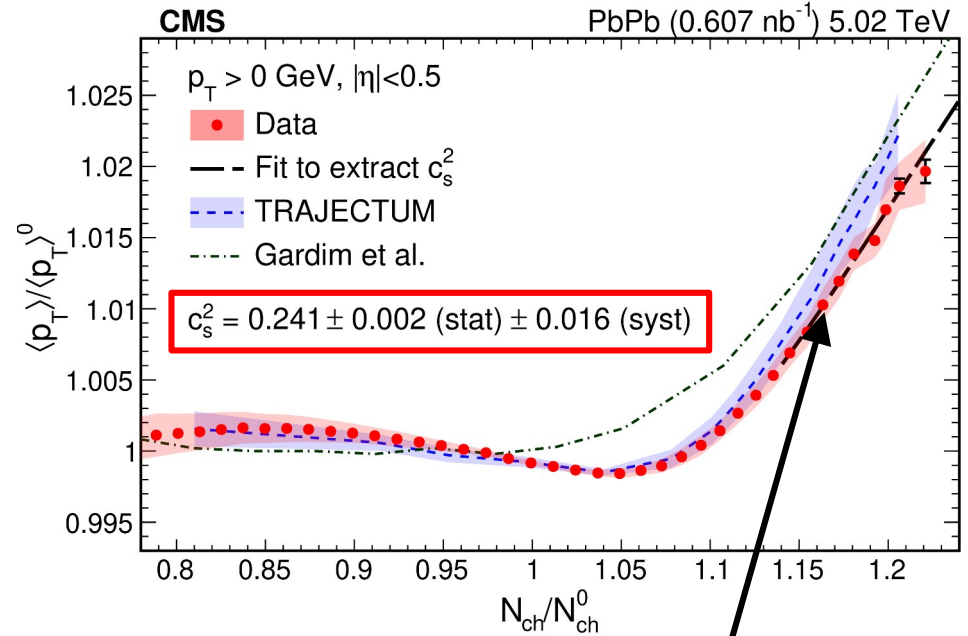


- c_s^2 can be extracted from $\langle p_T \rangle$ and N_{ch}
- Models predict a rising slope at large N_{ch}

Speed of sound in QGP



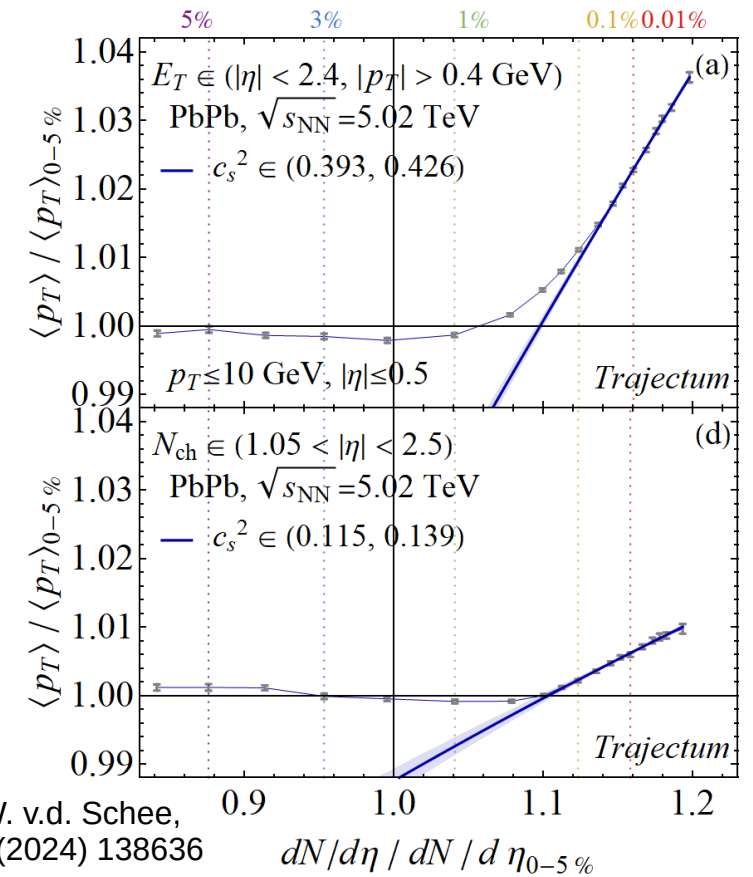
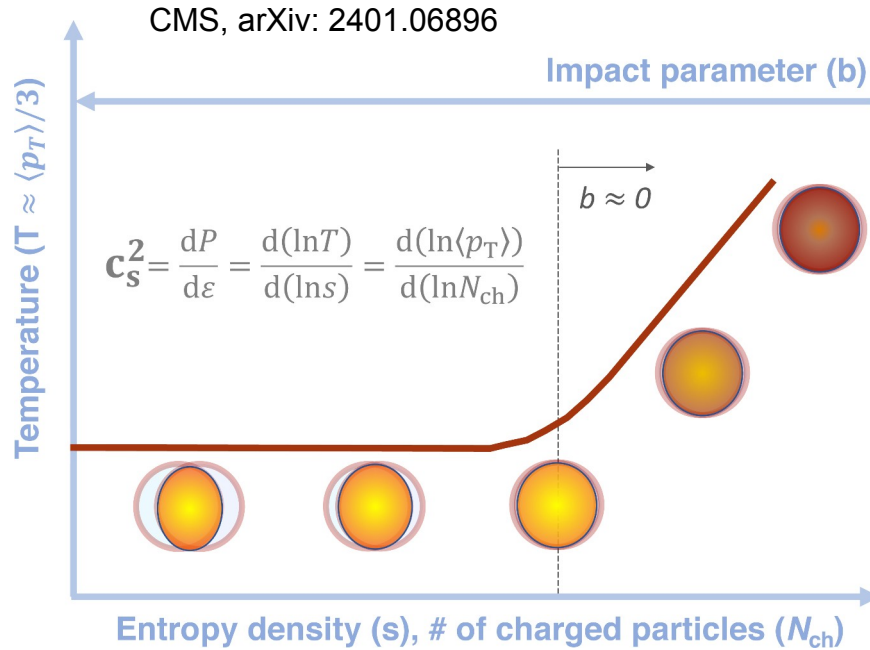
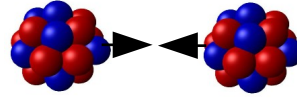
- c_s^2 can be extracted from $\langle p_T \rangle$ and N_{ch}
- Models predict a rising slope at large N_{ch}
 - Fit slope follows model calculations



$$\langle p_T \rangle^{\text{norm}} = \left(\frac{N_{ch}^{\text{norm}}}{\langle N_{ch}^{\text{knee}} | N_{ch}^{\text{norm}} \rangle} \right)^{c_s^2}$$

$$\langle N_{ch}^{\text{knee}} | N_{ch}^{\text{norm}} \rangle = N_{ch}^{\text{norm}} - \sigma \sqrt{\frac{2}{\pi}} \frac{\exp\left(-\frac{(N_{ch}^{\text{norm}} - \overline{N_{ch}^{\text{knee}}})^2}{2\sigma^2}\right)}{\text{erfc}\left(\frac{N_{ch}^{\text{norm}} - \overline{N_{ch}^{\text{knee}}}}{\sqrt{2}\sigma}\right)}$$

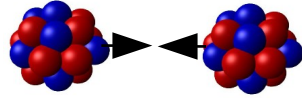
Speed of sound in QGP



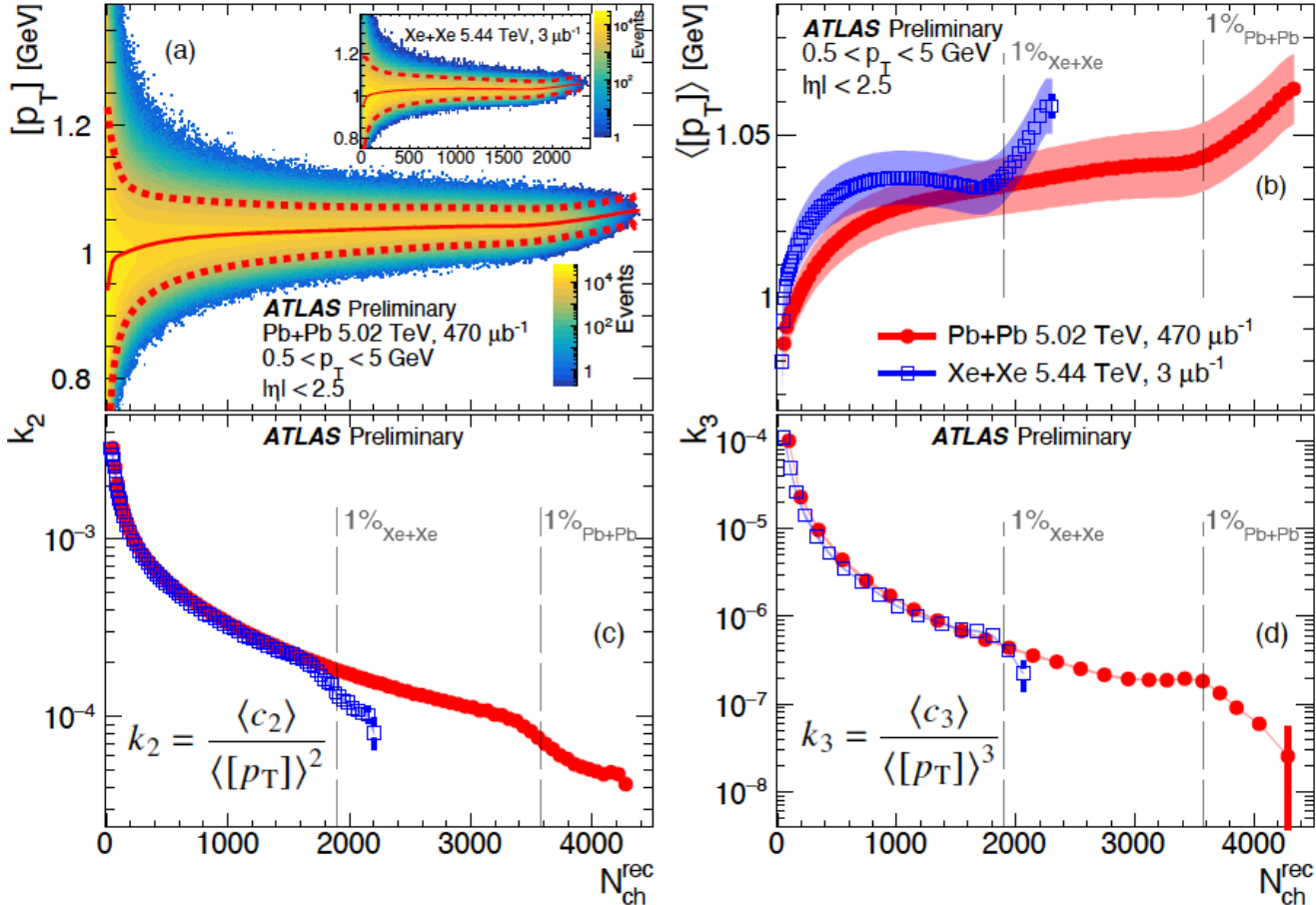
- c_s^2 can be extracted from $\langle p_T \rangle$ and N_{ch}
- Models predict a rising slope at large N_{ch}
 - Fit slope follows model calculations
- Ongoing discussions about any potential bias from centrality selection

$\langle p_T \rangle$ fluctuations

$$[p_T] = \frac{\sum_{i_1} w_{i_1} p_{T,i_1}}{\sum_{i_1} w_{i_1}}$$



ATLAS, CONF-2023-061

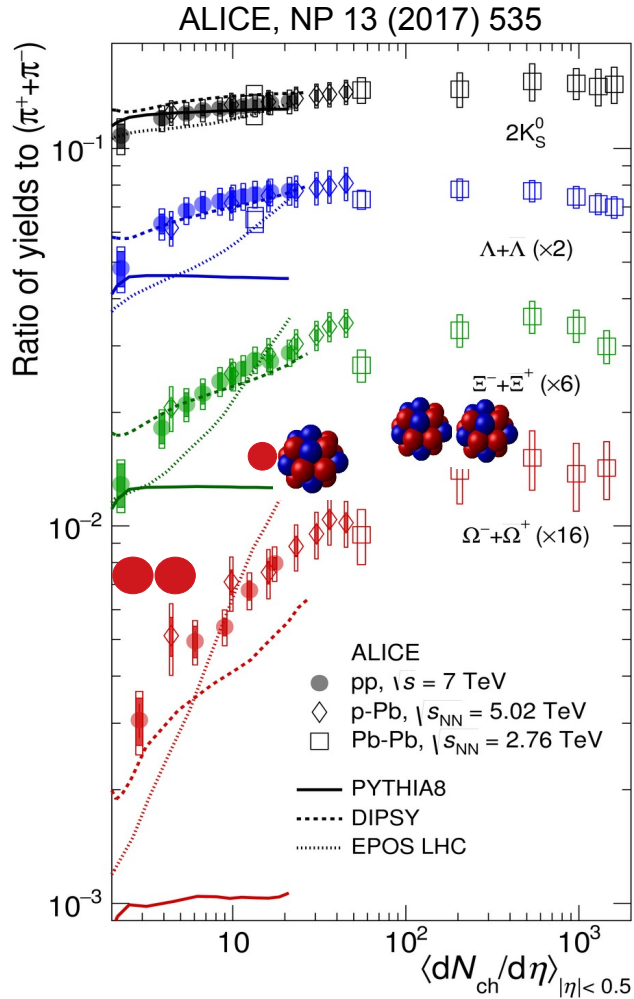


- Similar ATLAS measurement
 - Understand fluctuations in initial conditions
 - Geometric vs “intrinsic” fluctuations
 - Clear rise in $\langle [p_T] \rangle$ and drop in variance k_2
 - Expected from independent source models

R. Samanta et al., PRC 108 (2023) 024908
 R. Samanta et al., PRC 109 (2024) L051902

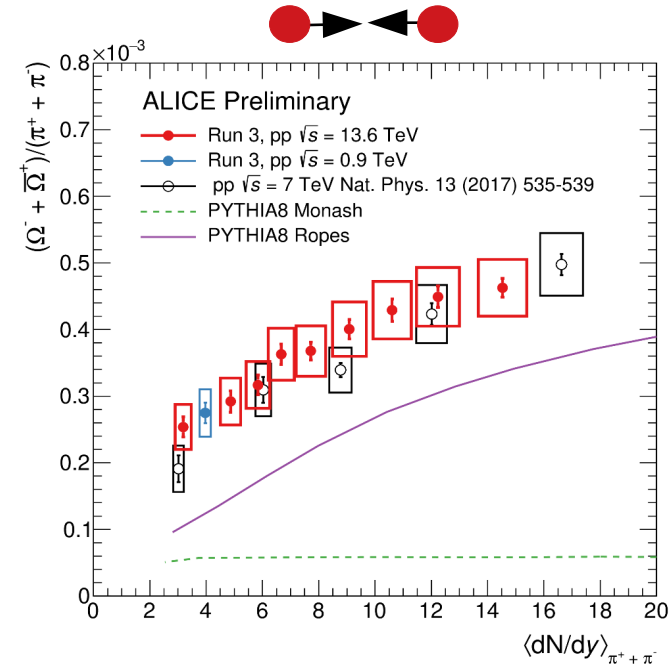
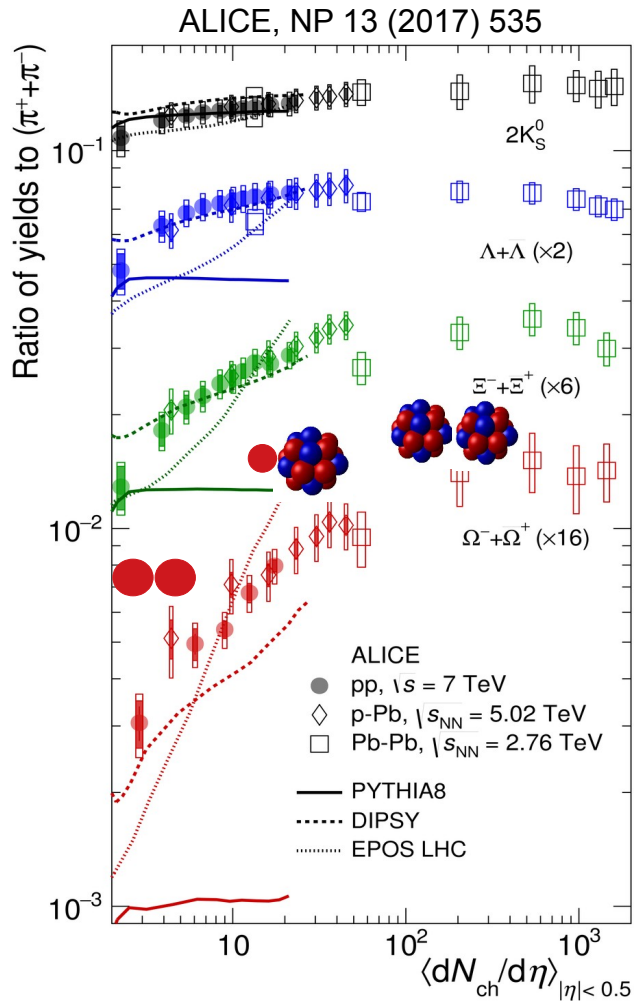
$$c_n = \frac{\sum_{i_1 \neq \dots \neq i_n} w_{i_1} \dots w_{i_n} (p_{T,i_1} - \langle [p_T] \rangle) \dots (p_{T,i_n} - \langle [p_T] \rangle)}{\sum_{i_1 \neq \dots \neq i_n} w_{i_1} \dots w_{i_n}}$$

Strangeness enhancement



- Strangeness increases with multiplicity
 - Hierarchy with strangeness content

Strangeness enhancement

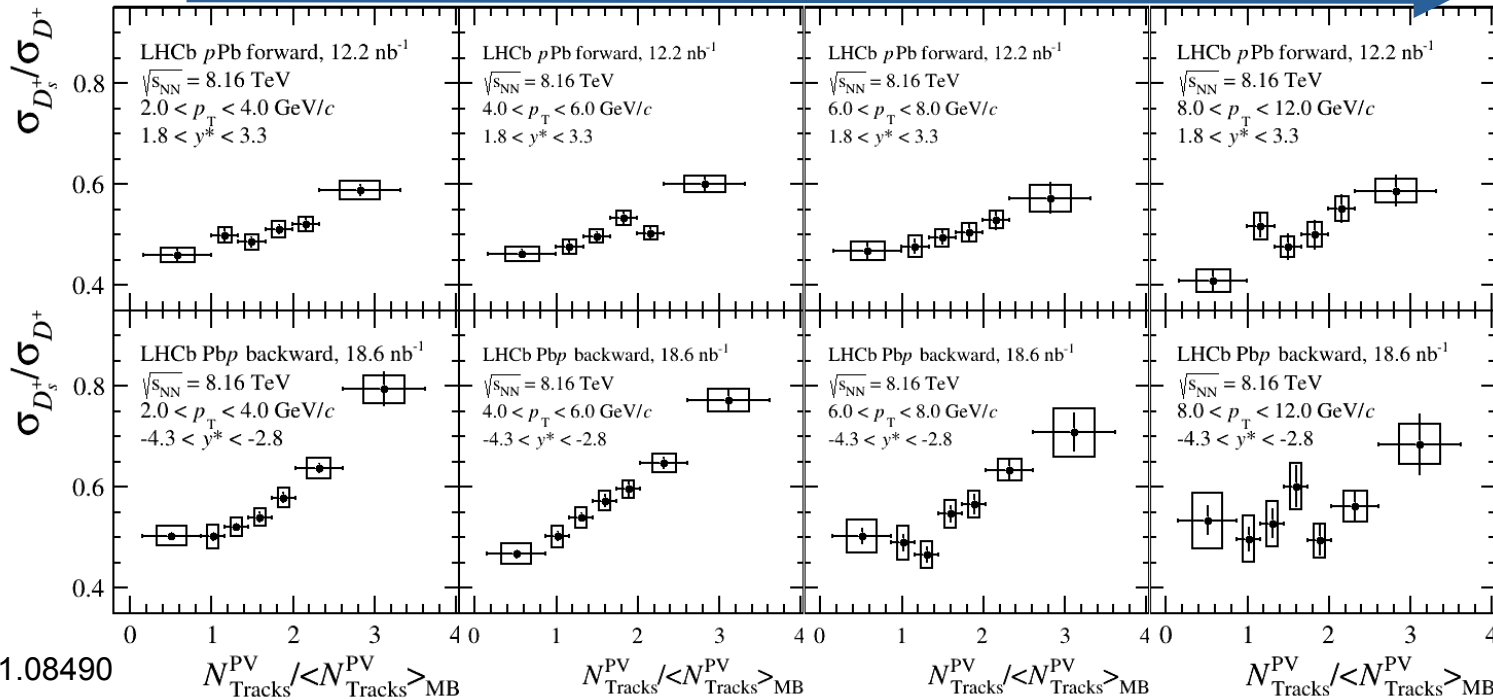


ALI-PREL-559079

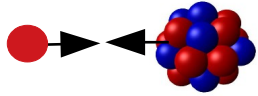
- Strangeness increases with multiplicity
 - Hierarchy with strangeness content
- More differential measurements in Run 3 → better constraints
 - pQCD-inspired models need extra mechanisms

Strangeness enhancement: charm

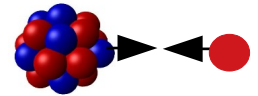
Increasing p_T →



Forward



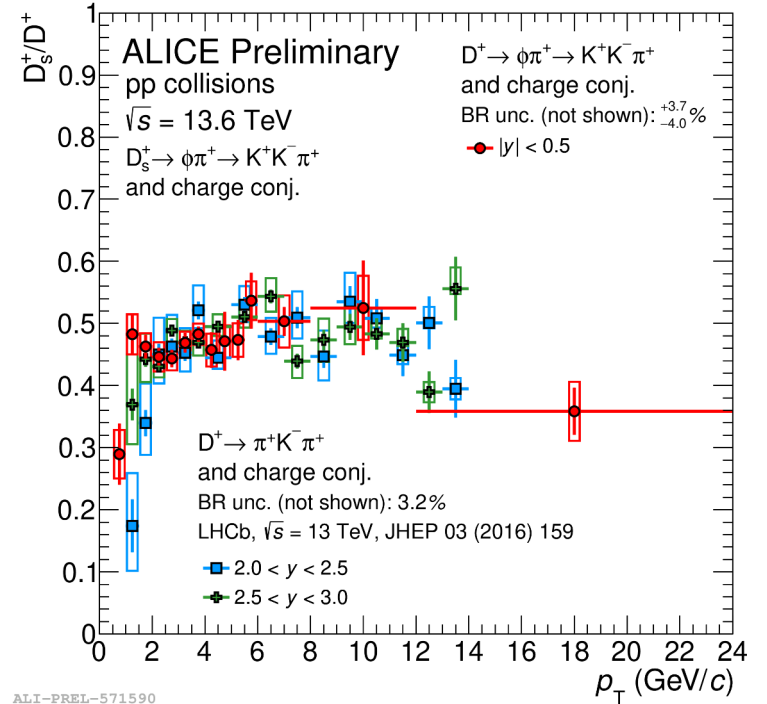
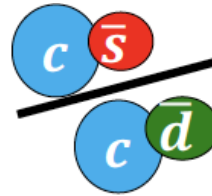
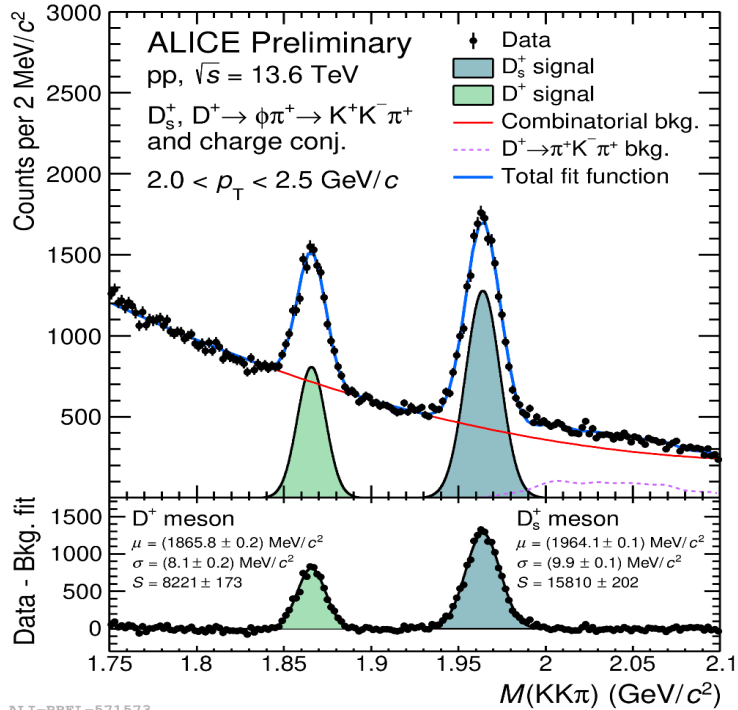
Backward



LHCb, arXiv: 2311.08490

- Compare D mesons with and without s quark
- Ratio increases with multiplicity at low p_T and backward rapidity → coalescence for charm hadronization
 - Strangeness enhancement observed in the charm sector

Strangeness enhancement: charm



- Compare D mesons with and without s quark
- Good agreement with LHCb results
- Investigate the multiplicity dependence

Summary

- QGP properties and phase diagram understood much better
 - Initial conditions
 - Equation of state
 - Transport coefficients
 - Particle production mechanisms
- Collectivity and strangeness enhancement in small systems
 - Develop new techniques and more differential measurements
 - Pushing the limits to understand the responsible mechanism(s)